UNITED NATIONS UNIVERSITY
UNU-GTP
Geothermal Training Programme

Orkustofnun, Grensasvegur 9,
IS-108 Reykjavik, Iceland

Reports 2017
Number 8

THE ASSESSMENT OF STEAM ABOVE GROUND SYSTEM OF UNIT-1 AND UNIT-2 ULUBELU GEOTHERMAL FIELD, INDONESIA, AFTER 5 YEARS OF OPERATION

Yanuaris Dwi Cahyono
PT Pertamina Geothermal Energy – PGE
Skyline Building 15th Floor, Jl. MH. Thamrin No.09
Jakarta
INDONESIA
yanuarisdwic@pertamina.com; yandwich@gmail.com

ABSTRACT

This study assesses the Steam Above Ground System (SAGS) of Unit-1 and Unit-2 in Ulubelu geothermal field in Indonesia after 5 years of operation. After this period of operation, there are changes in operation parameters such as pressure, temperature and flow from production wells due to the decline of the geothermal resource. It has effects not only on the SAGS performance, i.e. pressure drop, fluid velocity, equipment efficiency etc., but also potential silica scaling in the reinjection line. In addition, there is a reduction in the operating life of SAGS, especially regarding the pipes and the separator that need to be monitored and evaluated. This study focuses on pressure drop analysis of the two-phase flow of steam and brine, separator performance analysis, Silica Scaling Index (SSI) analysis in the reinjection line, wall thickness evaluation and estimation of turbine chamber pressure by Stodola's law. All of the calculations were done using Engineering Equation Solver (EES), comparing and evaluating both the design and the present condition. The assessment result shows that at present conditions, the SAGS performance decreases with the decrease of operation parameters. It is characterized by some operation parameters that are below allowable conditions, such as pressure and temperature at interface point, silica saturation index and steam quality at separator outlet. Based on those conditions, some optimization scenarios are recommended to be applied in order to improve the SAGS performance.

1. INTRODUCTION

The Ulubelu geothermal field is located in the administrative district of Tanggamus. It is about 100 km west of Bandar Lampung city, the capital city of Lampung Province in S-Sumatra, Indonesia. Geographically, the Ulubelu geothermal field is bounded by 104°27'25" and 104°43'31" east longitude and 5°15'16" and 5°31'29" south latitude. The total surface area of Ulubelu geothermal field is 90 ha (Figure 1).

The development of Ulubelu geothermal field began with an exploration stage that was conducted from 1991 to 2007. Activities undertaken at this stage include a survey of geology, geophysics, geochemistry,

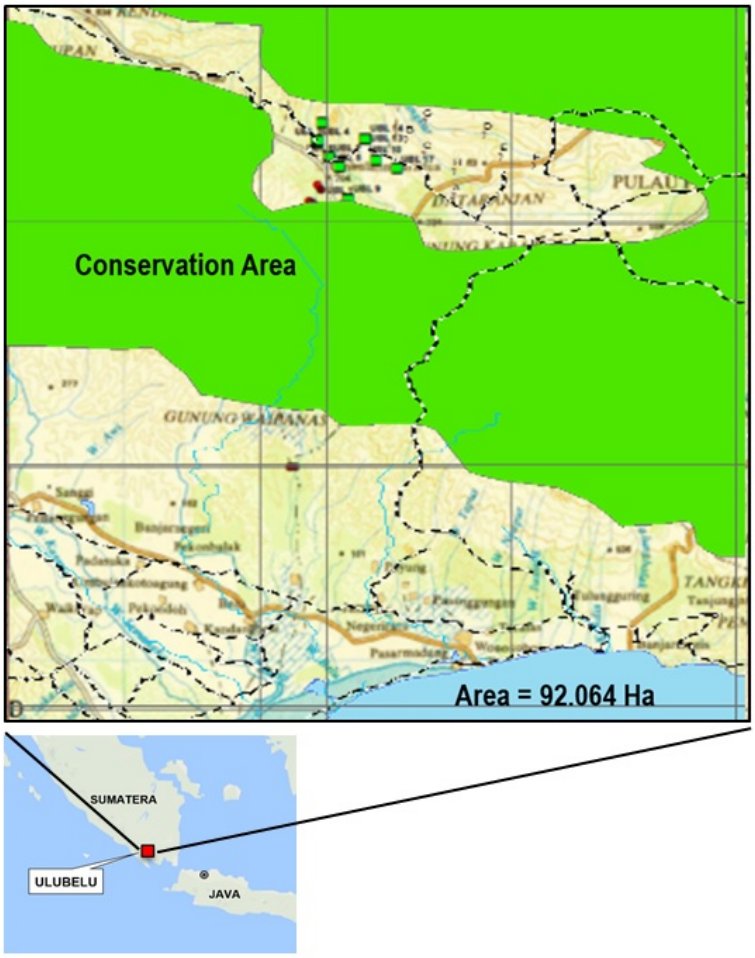

FIGURE 1: Location of the Ulubelu geothermal field (PGE, 2017a)

reservoir study and assessment, exploration drilling and land preparation. The next stage was the development stage, which was carried out from 2007 until 2012. The activities carried out were infrastructure development, delineation drilling of production and reinjection wells and construction of the steam above ground systems (SAGS) of Unit-1 and Unit-2. The production stage began in 2012 and has continued until today. In this stage, Unit-1 and Unit-2 started producing electricity with an installed capacity of 55 MW each. Parallel to operational activities of Unit-1 and Unit-2, two more units were developed, Unit-3 and Unit-4, each with an installed capacity of 55 MW. Production and monitoring activities of Unit-1 and Unit-2 were conducted in parallel with delineation drilling activities, as well as the engineering, procurement, construction and commissioning of the SAGS and Unit-3 and Unit-4 which were completed in the middle of 2017.

There are two business schemes of geothermal utilization in Ulubelu geothermal field. First, the steam sales contract (PJBU) for Unit-1 and Unit-2 and second, the electricity sales contract (PJBL) for Unit-3 and Unit-4. In the PJBU scheme, PT PERTAMINA Geothermal Energy (PT PGE) has a responsibility to build the SAGS and deliver steam to the power plant, which is owned by PT PLN (the State Electricity Company). In PJBL scheme, PT PGE has a responsibility to build SAGS and the power plant. The electricity from the power plant will be sold to PT PLN as the single buyer of electricity in Indonesia.

This paper will discuss SAGS of Unit-1 and Unit-2, which have been operating for 5 years, while Unit-3 and Unit-4 will not be discussed since those units started operation at the end of 2016 for Unit-3 and at the end of March 2017 for Unit-4. Therefore, the conditions of operating parameters and conditions of production facilities are still more or less the same as the design conditions and there has been no significant change in the short operation period.

1.1 Background and problems

The Ulubelu geothermal field is one of the geothermal fields in Indonesia that is characterized by two-phase fluids. The steam fraction in the total two-phase fluid is approximately 20% on average. The geothermal power plant of Unit-1 and Unit-2, which have been in operation since 2012, is supplied from three production well clusters and two reinjection well clusters (Figure 2). Distribution of production wells and reinjection wells for Unit-1 and Unit-2 is as follows:

Production well clusters

1. Cluster-B, consists of four wells:
   - UBL-02 (B1)
   - UBL-03 (B2)
   - UBL-15 (B4)
   - UBL-16 (B5)
2. Cluster-C, consists of four wells:
   - UBL-05 (C1)
   - UBL-06 (C2)
   - UBL-07 (C3)
   - UBL-08 (C4)
3. Cluster-D,consists of three wells:
   - UBL-11 (D1)
   - UBL-12 (D2)
   - UBL-14 (D4)

Reinjection well clusters

1. Cluster A, consists of three wells:
   - UBL-01 (A1)
   - UBL-18 (A3)
   - UBL-23 (A4)
2. Cluster F, consists of three wells:
   - UBL-17 (F1)
   - UBL-19 (F2)
   - UBL-23 (F3)

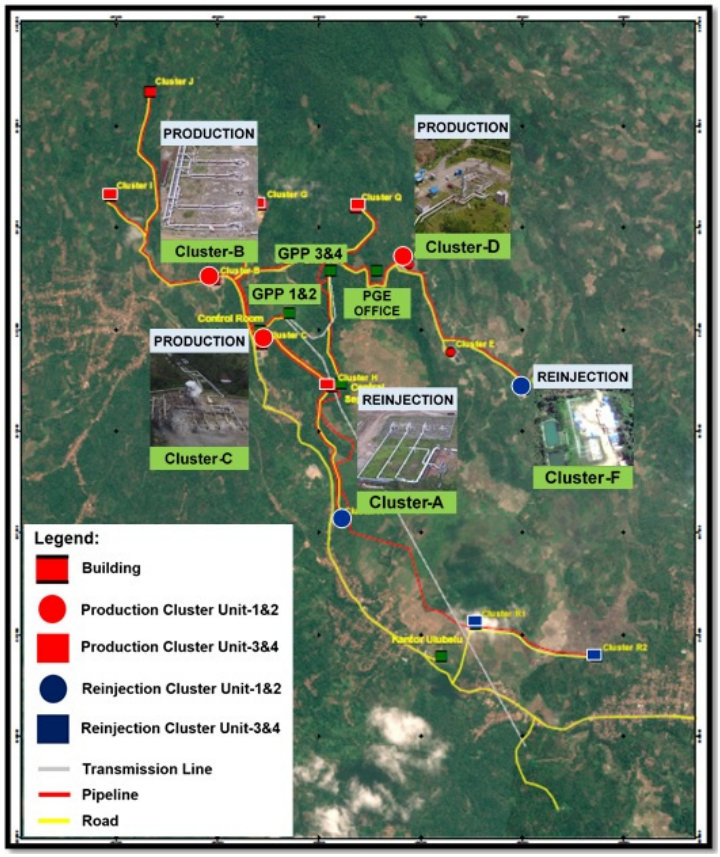

FIGURE 2: Cluster layout of Unit-1 and Unit-2, Ulubelu geothermal field (PGE, 2017a)

During the operation of approximately five years from 2012 to 2017, where the operating parameters in SAGS were routinely monitored, locally or in the control room, some changes have been observed. The experienced changes are for example, decrease of pressure, temperature and production capacity due to a decline in well performance, and the reduced operating life of production facilities such as pipes and separators. The current condition are much different from the current state of the SAGS at design conditions that is the start of the operation. Another important issue is the potential for scaling in pipelines, especially in the brine pipeline from the production separator to the reinjection wells due to the decline in operating parameters.

1.2 Objectives of the study

The main objective of this study is to assess the SAGS of Unit-1 and Unit-2 Ulubelu geothermal field after 5 years of operation, regarding problems that were stated in Section 1.1. The specific objectives to achieve the main objective are:

1. To compare, analyse and evaluate the performance of the SAGS of Unit-1 and 2 at Ulubelu geothermal field between the design condition and actual condition after operation for 5 years;
2. To give a recommendation about SAGS optimization and future strategy of its operation;
3. To make a template of the SAGS assessment for the next assessment activity, since this is the first assessment of it.

1.3 Scope and limitations of the study

Design data will be used as the basic data to compare with the calculation results. This data is the engineering data of SAGS Unit-1 and Unit-2 in Ulubelu geothermal field before the construction phase. However, due to the limitations of the basic data, this study focuses on:

1. Mechanical parameters, specifically on the pipeline and separator thickness monitoring and evaluation using wall thickness measurement data after the start of operation of SAGS Unit-1 and Unit-2 until early 2017
2. Process parameters, specifically calculations of pressure drops in the two-phase flow, steam and brine, two-phase flow patterns and separator performance. These calculations use actual data that are monitored from the central control room of SAGS Unit-1 and Unit-2 until early 2017; and
3. Chemical parameters, specifically calculation of the silica scaling index (SSI) in the reinjection line from the separators to reinjection wells. Chemical data was taken from the laboratory of Ulubelu geothermal field in early 2017.

Definitions on parameters are given in the Nomenclature section towards the end of the report.

2. OVERVIEW OF STEAM ABOVE GROUND SYSTEM (SAGS) OF UNIT-1 AND UNIT-2

2.1 General data

The general data, which are used to support the calculations, both at the design condition and present condition are as follows (PGE, 2012):

1. *Barometric pressure due to elevation of each cluster:*
   - Cluster-A : 0.9320 bar-a (703.12 m a.s.l.)
   - Cluster-B : 0.9155 bar-a (853.44 m a.s.l.)
   - Cluster-C : 0.9256 bar-a (760.90 m a.s.l.)
   - Cluster-D : 0.9194 bar-a (817.43 m a.s.l.)
   - Cluster-F : 0.9309 bar-a (712.58 m a.s.l.)
   - Interface point : 0.9235 bar-a (780 m a.s.l.)
2. *Air temperature:*
   - Maximum : 34°C
   - Minimum : 22.3°C
   - Average (annually) : 26.7°C
3. *Air relative humidity:*
   - Maximum : 97%
   - Minimum : 60%
   - Average : 83%
4. *Rainfall:*
   - Maximum (annually) : 2850 mm
   - Minimum (annually) : 630 mm
   - Average (annually) : 1899 mm
5. *Wind:*
   - Maximum velocity : 2.94 m/s
   - Average velocity : 2 m/s
6. *Seismicity:*
   According to zone 5 Indonesian Code SNI 03-1726-2002 it is 0.3 G

2.2 Steam availability (based on discharge test results)

The main purpose of discharge tests is to get information about the potential energy output of geothermal wells in MW before they are used to supply steam to the power plant. This activity is done after drilling and the heating up of the well. In Ulubelu geothermal field, discharge tests were carried out between 2010 and 2011 before the construction phase of the SAGS and the power plant began by using the

separator method. The separator method has the highest accuracy compared with other methods, such as the Lip pressure method, with accuracy level at the normal control of flow ± 4%; enthalpy ± 30 kJ/kg and at the careful control of flow ± 2%; enthalpy ±10 kJ/kg (Grant et al., 1982). Geothermal wells in Ulubelu are non-artesian wells, meaning that the well cannot discharge by itself so they need stimulation to discharge, mostly by using an air compression system (Mubarok and Zarrouk, 2017). Figure 3 shows the results from discharge tests for production wells of Unit-1 and Unit-2 which are expressed in deliverability curves of flow and enthalpy as a function of wellhead pressure.

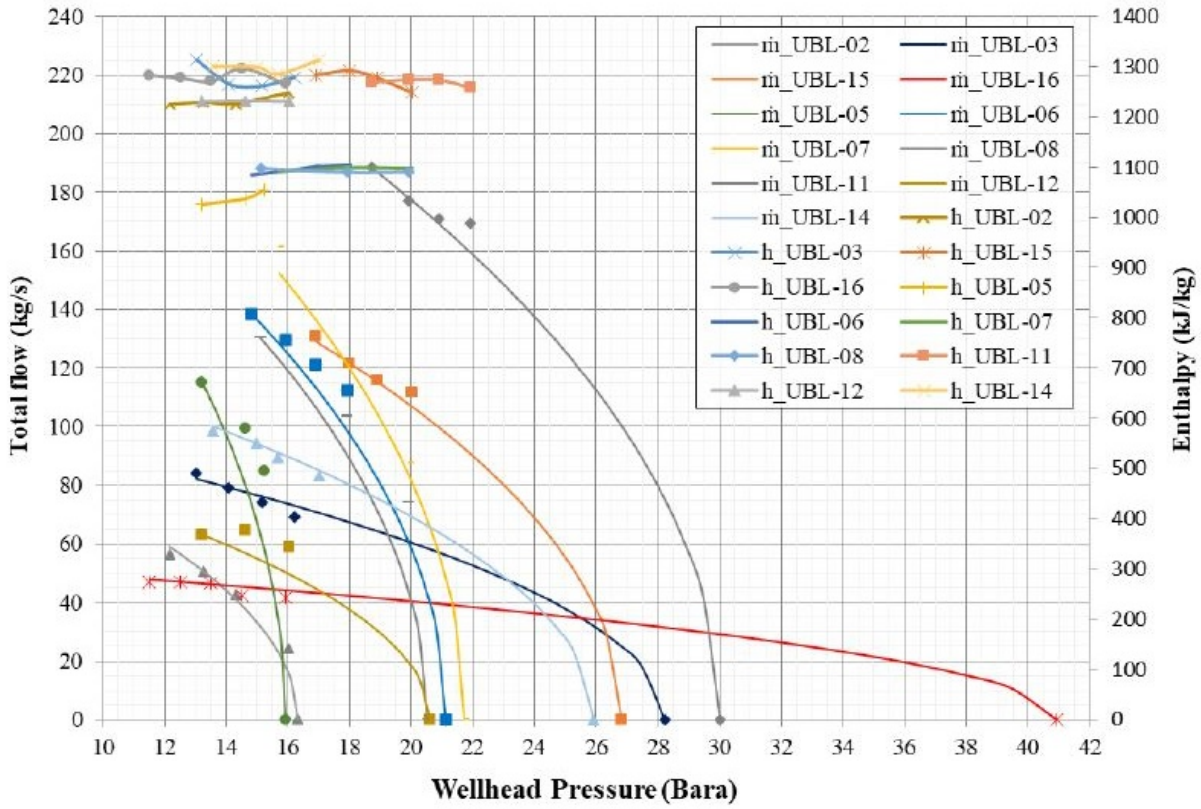

FIGURE 3: Deliverability curve of production wells of Unit-1 and Unit-2 Ulubelu (PGE, 2011)

Steam availability for Unit-1 and Unit-2 based on discharge test results at design operation condition is shown in Table 1. As mentioned above, 11 production wells and 6 reinjection wells are used in SAGS Unit-1 and Unit-2 with total steam availability of 839 ton/h or 2323 kg/s, average enthalpy 1208 kJ/kg and average steam fraction 20.9%. Those amounts of steam are sufficient to generate electricity in two 55 MW units by using the assumption of specific

TABLE 1: Steam availability of Unit-1 and 2 Ulubelu (PGE, 2012)

Wells	WHP (bar-a)	Mass flow (Ton/h)	Mass flow (kg/s)	Enthalpy (kJ/kg)	Steam fraction (%)
Cluster-B					
UBL-2 (B1)	11.75	287.50	79.86	1253.60	23.12
UBL-3 (B2)	11.75	303.60	84.33	1283.90	24.62
UBL-15 (B4)	11.79	438.20	121.72	1280.10	24.38
UBL-16 (B5)	11.79	300.00	83.33	1253.50	23.08
Cluster-C					
UBL-5 (C1)	10.31	330.00	91.67	1045.70	13.77
UBL-6 (C2)	10.33	350.00	97.22	1102.50	16.58
UBL-7 (C3)	10.33	451.00	125.28	1102.50	16.58
UBL-8 (C4)	10.30	330.00	91.67	1099.20	16.44
Cluster-D					
UBL-11 (D1)	12.90	652.10	181.14	1271.80	23.23
UBL-12 (D2)	12.90	232.40	64.56	1233.60	21.32
UBL-14 (D4)	12.90	354.80	98.56	1302.60	24.79

steam consumption 7 ton/h per MW or 1.94 kg/s per MW. This assumption was made based on general data of interface point pressure in the steam sales contract (PJBU) between PGE and PLN. This is also considered when selecting wellhead pressure for each production well.

2.3 Process flow diagram and heat mass balance at design condition

The process flow diagram in Figure 4 describes the flow sequence of the fluid from the wellhead to the steam interface point. The heat mass balance (HMB) in Table 2 shows the value of the operation parameters at each point starting from the two-phase line after the wellhead to the steam interface point. The interface point is the limit area between the SAGS, which is operated by PT PGE and the power plant, which is operated by PT PLN.

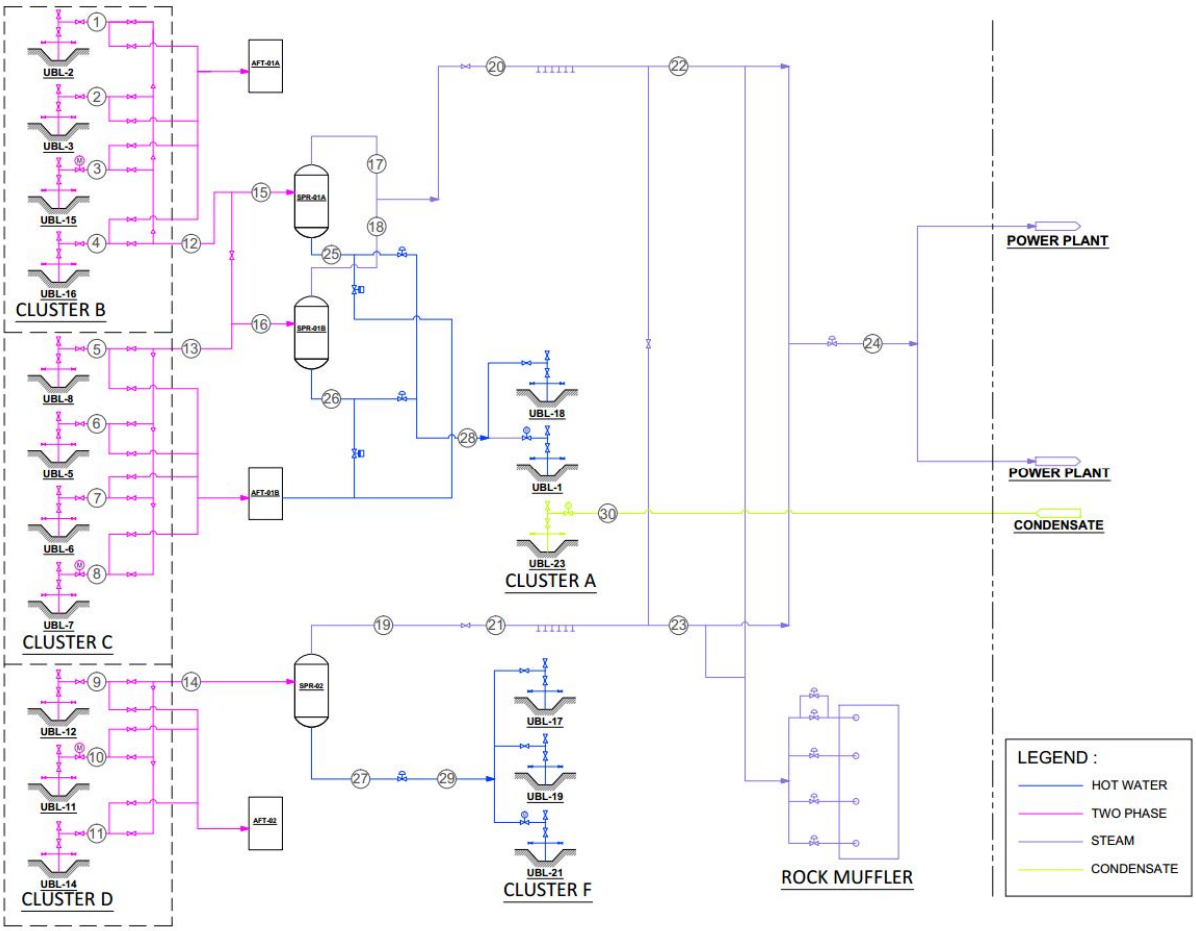

FIGURE 4: Process flow diagram of SAGS Unit-1 and Unit-2, Ulubelu (PGE, 2012)

The general process description of the process flow diagram is divided into three sections as below:

1. Two-phase line

The two-phase geothermal fluid is flowing from three different production clusters, Cluster-B with four production wells (UBL-02, 03, 15 and 16), Cluster-C with four production wells (UBL-05, 06, 07 and 08) and Cluster-D with three production wells (UBL-11, 12 and 14). The two-phase fluid from each well flows through a 12" diameter pipeline to the two-phase header in each cluster. A header with larger size of diameter (30-36") collects two-phase fluid from the wells. From the header it flows to the separator where steam and brine are separated. The two-phase fluid from Cluster-B flows to Separator-01A, which is located about 1.3 km away in Cluster-C, the two-phase fluid from Cluster-C flows to Separator-01B, which is located close to the production wells, while two-phase fluid from Cluster-D

TABLE 2: Heat mass balance of SAGS Unit-1 and Unit-2 Ulubelu at design condition

Stream number		1	2	3	4	5	6	7	8	9	10
Fluid properties	Units	CLUSTER-B				CLUSTER-C				CLUSTER-D	
		2 ϕ from UBL-02	2 ϕ from UBL-03	2 ϕ from UBL-15	2 ϕ from UBL-16	2 ϕ from UBL-08	2 ϕ from UBL-05	2 ϕ from UBL-06	2 ϕ from UBL-07	2 ϕ from UBL-12	2 ϕ from UBL-11
Pressure	bar-a	11.75	11.75	11.79	11.79	10.30	10.31	10.33	10.33	12.90	12.90
Temperature	°C	186.90	187.01	187.27	187.03	181.27	181.31	181.41	181.41	191.27	191.41
Mass flow	Ton/h	287.50	303.60	438.20	300.00	330.00	330	350.00	451.00	232.40	652.10
	kg/s	79.86	84.33	121.72	83.33	91.67	91.67	97.22	125.28	64.56	181.14
Enthalpy	kJ/kg	1253.60	1283.90	1280.10	1253.50	1099.20	1045.70	1102.50	1102.50	1233.60	1271.80
Steam fraction	%	23.12	24.62	24.38	23.08	16.44	13.77	16.58	16.58	21.32	23.23
Stream number		11	12	13	14	15	16	17	18	19	20
Fluid properties	Units	CLUSTER-D									
		2 ϕ from UBL-14	2 ϕ from Cluster-B	2 ϕ from Cluster-C	2 ϕ from Cluster-D	2 ϕ Cluster-B	2 ϕ Cluster-C	Steam at Cluster-B	Steam at Cluster-C	Steam at Cluster-D	Steam
Pressure	bar-a	12.90	10.43	10.30	12.61	10.20	9.98	9.77	9.73	12.31	9.16
Temperature	°C	191.41	181.68	181.26	190.31	180.69	179.89	178.81	178.79	189.20	177.46
Mass flow	Ton/h	354.80	1329.30	1461.00	1239.30	1329.30	1461.00	337.71	240.10	294.24	577.81
	kg/s	98.56	369.25	405.83	344.25	369.25	405.83	93.81	66.69	81.73	160.50
Enthalpy	kJ/kg	1302.60	1269.90	1088.90	1273.70	1270.10	1089.20	2776.70	2776.70	2784.80	2775.60
Steam fraction	%	24.79	24.86	15.93	23.52	25.05	16.21	100.00	100.00	100.00	100.00
Stream number		21	22	23	24	25	26	27	28	29	30
Fluid properties	Units	Steam	Steam	Steam	Steam to GPP	Hot brine to Clust. A	Hot brine to Cluster-A	Hot brine to Cluster-F	Hot brine at Cluster-A	Hot brine at Cluster-F	Condensate to Clust.-A
Pressure	bar-a	9.19	9.09	9.09	8.00	9.77	9.73	12.31	10.47	18.98	14.30
Temperature	°C	176.51	176.33	175.78	174.20	178.81	178.79	189.20	178.36	188.48	50.00
Mass flow	Ton/h	294.14	447.00	424.87	871.90	991.59	1220.90	945.06	2212.49	945.06	290.40
	kg/s	81.71	124.17	118.02	242.19	275.44	339.14	262.52	614.58	262.52	80.67
Enthalpy	kJ/kg	2774.70	2774.50	2773.80	2771.90	757.80	757.70	803.90	755.80	800.70	209.30
Steam fraction	%	100.00	100.00	100.00	100.00	0.00	0.00	0.00	0.00	0.00	0.00

flows to Separator-02 which is also located close to the production wells. The separation process of two-phase fluid uses centrifugal force. The brine which has a higher density will fall down and flows to the brine line and onwards to reinjection wells while the steam with lower density goes up and flows to the steam line.

2. Steam line

After the two-phase flow has been separated, steam from Separator-01A and Separator-01B in Cluster-C goes through a 30" diameter pipeline to the header. From there, steam from the two separators goes to the interface point to be joined with the steam from Separator-02 in Cluster-D and then to the power plant. In the steam line, there is a scrubbing line with a larger diameter to trap condensed steam in the pipeline and drain it to the atmosphere through a steam trap. There is also a rock muffler to vent excess steam or steam that is not being used by the power plant. It also has the function of venting steam during load rejection or a power plant trip. Steam pressure at the interface point is maintained as required by the power plant.

3. Brine line

Brine is another product of the separation and it goes to two reinjection well clusters. Brine from Separator-01A and Separator-01B goes to reinjection wells in Cluster-A (UBL-01 and 09) and brine from Separator-02 goes to reinjection wells in Cluster-F (UBL-17, 19 and 21). The brine is reinjected by gravity or by using separator pressure and elevation difference between the separator and reinjection wells. Besides that, one reinjection well, specifically UBL-23 in Cluster-A, is used as a reinjection well for condensate water from the power plant. Centrifugal pumps are used to pump the condensate from the cooling tower basin to the reinjection well at a low temperature.

2.4 Pipeline data and specification

Most of the production facilities used in SAGS of Unit-1 and 2 are pipes. These pipes are used starting from wellhead to interface point. The specification of the pipe depends on the type of application in each section, for example, a pipe for two phases will have different specifications with pipes for steam and brine. Many factors have an influence on it, such as operating pressure and temperature, fluid flow rate, the chemical composition of the fluid, etc. Figure 5 shows the schematic diagram of SAGS of Unit-1 and Unit-2 (PGE, 2012).

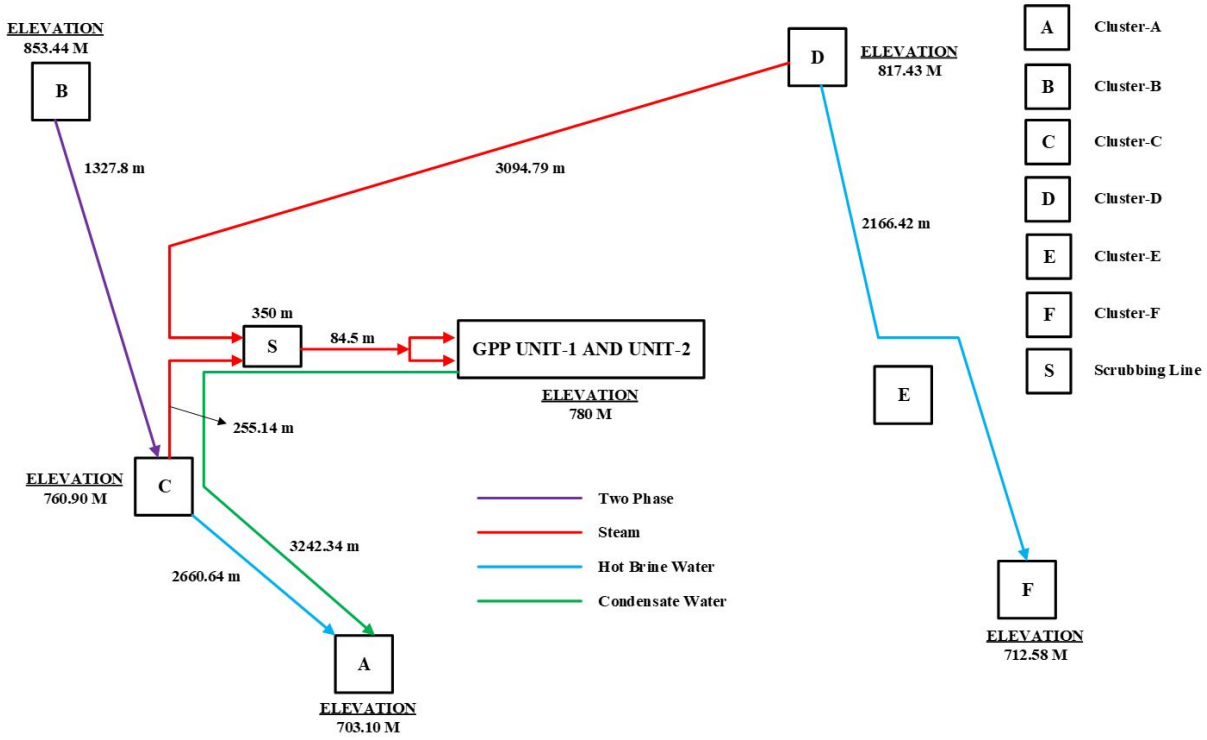

FIGURE 5: The schematic diagram of SAGS Unit-1 and Unit-2 Ulubelu

Table 3 below shows the classification of pipelines depending on what they are used for. Design pressure is determined based on the maximum limit of operating pressure for the classification of each class, based on the operational condition in each pipeline.

TABLE 3: Classification of mainline service (PGE, 2012)

No	Line service	Area	P_O (bar-g)	P_D (bar-g)	T_D (°C)	Pipe class
1	Well branchline (high pressure)	All clusters	-	60	296	T3
2	Two-phase line	Test line	-	25	215	T2
	(medium pressure)	Cluster-D	12.58	14.1	215	T2
3	Two-phase line	Cluster-B	11.4	12.8	210	T1
	(low pressure)	Cluster-C	9.98	11.5	205	T1
4	Steam line	D - GPP	11.96	13.5	210	S1
		C - GPP	9.31	10.8	200	S1
5	Hot brine	D - F	18.62	20.4	210	B2
		C - A	10.86	13.4	197	B2
6	Condensate	GPP - A	14.3	16	70	C1

The data and specifications of the pipes are determined based on process and pipeline modelling during the design phase. These results will be the same as the actual data for the pipes. When the pipes are

selected, many parameters, such as the diameter, material, thickness, etc. have to be considered. The tolerances were applied to ensure the safety of the pipes during the operation phase. The data and the specification of the pipes are shown in Table 4.

TABLE 4: Pipe data and specifications of SAGS of Unit-1 and Unit-2 in Ulubelu

From	To	Stream no.	Piupe length (m)	Pipe specification	Pipe OD (")	Pipe ID (")	Pipe thickness (mm)	Insulation thickness (mm)
2 Phase UBL-02	2 Phase Header Cluster-B	1	18.39	ANSI B31.1 - 600#	12.75	11.37	17.48	50.8
2 Phase UBL-03	2 Phase Header Cluster-B	2	19.07	ANSI B31.1 - 600#	12.75	11.37	17.48	50.8
2 Phase UBL-15	2 Phase Header Cluster-B	3	22.36	ANSI B31.1 - 600#	12.75	11.37	17.48	50.8
2 Phase UBL-16	2 Phase Header Cluster-B	4	21.92	ANSI B31.1 - 600#	12.75	11.37	17.48	50.8
2 Phase Header Cluster-B	TP#1 Cluster-C	12	1327.8	ANSI B31.1 - 150#	36	35.17	10.31	50.8
2 Phase UBL-08	2 Phase Header Cluster-C	5	24.65	ANSI B31.1 - 600#	12.75	11.37	17.48	50.8
2 Phase UBL-05	2 Phase Header Cluster-C	6	23.2	ANSI B31.1 - 600#	12.75	11.37	17.48	50.8
2 Phase UBL-06	2 Phase Header Cluster-C	7	22.68	ANSI B31.1 - 600#	12.75	11.37	17.48	50.8
2 Phase UBL-07	2 Phase Header Cluster-C	8	27.92	ANSI B31.1 - 600#	12.75	11.37	17.48	50.8
2 Phase Header Cluster-C	TP#1 Cluster-C	13	3.7	ANSI B31.1 - 150#	36	35.17	10.31	50.8
TP#1 Cluster-C	SEP-01A Cluster-C	15	20	ANSI B31.1 - 150#	36	35.17	10.31	50.8
TP#1 Cluster-C	SEP-01B Cluster-C	16	27	ANSI B31.1 - 150#	36	35.17	10.31	50.8
1 Phase Sep-01A	Steam Header Sep-01A	17	30.3	ANSI B31.1 - 150#	30	29.25	9.53	50.8
Hot brine Sep-01A	Tie in Sep-01A	25	36	ANSI B31.1 - 300#	16	15.31	8.74	25
1 Phase Sep-01B	Steam Header Sep-01B	18	30.3	ANSI B31.1 - 150#	30	29.25	9.53	50.8
Hot brine Sep-01B	Tie in Sep-01B	26	40.72	ANSI B31.1 - 300#	18	17.31	8.74	25
Tie in hot brine Sep-01A/B	Cluster-A1	28	2660.64	ANSI B31.1 - 300#	28	27.3	8.74	25
Steam Header Sep-01A/B	Scrubbing Line#1	20	207.3	ANSI B31.1 - 150#	42	41.2	10.31	50.8
Scrubbing Line#1	Gathering station	22	397.84	ANSI B31.1 - 150#	48	47.12	11.13	50.8
2 Phase UBL-12	2 Phase Header Cluster-D	9	46.8	ANSI B31.1 - 600#	12.75	11.37	17.48	50.8
2 Phase UBL-11	2 Phase Header Cluster-D	10	34.3	ANSI B31.1 - 600#	12.75	11.37	17.48	50.8
2 Phase UBL-14	2 Phase Header Cluster-D	11	30.5	ANSI B31.1 - 600#	12.75	11.37	17.48	50.8
2 Phase Header Cluster-D	SEP-02 Cluster-D	14	77.26	ANSI B31.1 - 300#	30	29.25	9.53	50.8
Hot brine Sep-02	Cluster-F	27	2166.42	ANSI B31.1 - 300#	20	19.25	9.53	25
1 Phase TP#2 Cluster-D	Balancing Line	19	3094.79	ANSI B31.1 - 150#	30	29.25	9.53	50.8
Balance Line	Scrubbing Line#2	21	153	ANSI B31.1 - 150#	28	27.25	9.53	50.8
Scrubbing Line#2	Gathering station	23	350	ANSI B31.1 - 150#	48	47.12	11.13	50.8
Gathering station	Interface point	24	56.11	ANSI B31.1 - 150#	52	51.13	11.13	50.8
Condensate water	Cluster-A2	30	3242.34	ANSI B31.1 - 150#	12.75	12.09	8.30	25

Note :
- Insulation material is calcium silicate, k = 0.075 W/m-K and aluminium sheet, k = 240.84 W/m-K
- Pipe roughness is 0.045 mm, k-pipe = 48.64 W/m-K

2.5 Separator data

In the SAGS of Unit-1 and Unit-2 there are three production separators; Separator-01A and 01B are located in Cluster-C and Separator-02 is located in Cluster-D. All have the same dimensions but different specifications, because the inlet and operating conditions, such as pressure, temperature, enthalpy, steam quality and two-phase flow are different for each cluster. Separators 01A and 01B are used to accommodate two-phase fluids from production wells in Cluster-B and Cluster-C, while Separator-02 is used to accommodate two-phase fluids from Cluster-D. All separators in Ulubelu are of the vertical Webre-cyclone type, using centrifugal force to separate the two-phase fluid. After flowing to the separator, the two-phase fluid will rotate several times, fluid with higher density will fall down and goes to the brine line at bottom, and steam with lower density will go up to the top side and flow through the steam line.

The separators have an integral water drum and the brine collected there will be discharged through the level control valve. An emergency dump valve with automatic stroking is installed in the brine line in case the water level inside the water drum is too high, and the fluid is discharged through an atmospheric

flash tank (AFT). A level gauge and a controller are connected to the separator to indicate the level of fluid inside the water drum. During operation, the separator pressure shall be kept constant by vent valves that discharge steam to the venting system or rock muffler. Table 5 shows general data for separators in the SAGS of Unit-1 and Unit-2.

TABLE 5: General data for separators in Unit-1 and Unit-2, Ulubelu (PGE, 2012)

Parameter	Symbol	Units	Design data		
			Separator-01A	**Separator-01B**	**Separator-01**
Type			Vertical Webre Cyclone		
Fluid			Steam and Brine		
Pressure	P	Bar-g	9.18	8.96	11.75
Temperature	T	ºC	180.70	179.90	190.90
Total flow	M	Ton/h	1329.30	1466.00	1239.30
		kg/s	369.25	407.22	344.25
Mixture enthalpy	h	kJ/kg	1270.00	1089.00	1270.00
Mass flow rate of steam	M_V	Ton/h	332.95	237.47	290.12
		kg/s	92.49	65.96	80.59
Mass flow rate of brine	M_L	Ton/h	996.35	1228.35	949.18
		kg/s	276.76	341.21	263.66
Steam inlet quality	X	%	25.05	16.20	23.41
Pressure drop (allowable)	ΔP	Bar-g	0.47	0.23	0.30
Volume flow of steam	Q_V	m^3/h	64366.39	47125.61	45451.56
Volume flow of brine	Q_L	m^3/h	1140.01	1404.00	1099.20
Enthalpy of steam	h_V	kJ/kg	2778.30	2777.60	2785.50
Enthalpy of brine	h_L	kJ/kg	766.10	762.50	811.40
Density of steam	ρ_V	kg/m^3	5.17	5.04	6.38
Density of brine	ρ_L	kg/m^3	873.98	874.78	863.51
Specific volume of steam	V_V	m^3/kg	0.1933	0.1983	0.1567
Specific volume of brine	V_L	m^3/kg	0.0011	0.0011	0.0012
Viscosity of steam	μ_V	cP	0.012	0.012	0.001
Viscosity of brine	μ_L	cP	0.149	0.149	0.140
Mol weight of steam			18.30	18.30	18.10
Mol weight of brine			18.00	18.00	18.00
Surface tension of brine	σ_L	dyne/cm	42.12	42.30	39.86

3. BASIC THEORY

3.1 Single-phase flow

In this study of the SAGS of Unit-1 and Unit-2 in Ulubelu, the single-phase flow in the pipe is steam or brine. The steam flows from the separated steam line in the separator to the interface point close to the power plant. The steam is used to generate electricity in the power plant which has two units of 55 MW each. The brine flows from the separated brine line in the separator to the reinjection wells by gravity. In addition, there is also the condensate from the power plant, which is produced by a condensation process of the steam in the condenser. The condensate is pumped to the reinjection well, where it has a fairly low temperature. Parameters used in the equations below are defined in the Nomenclature at the back of the report.

In the single-phase flow, a pressure drop that occurs in the pipe is due to friction along the pipe and the elevation difference (Purwono, 2010). Pressure drop due to friction can be predicted by calculating the velocity of single-phase fluid in the pipeline using:

$$v = \left(\frac{4\,Q}{\pi\, ID^2}\right) \tag{1}$$

IPS (1996) explained that the velocity range of single-phase flow in the pipe for water is maximum 3 m/s, and for steam it is maximum 40 m/s (saturated steam) and 60 m/s (superheated steam). This velocity limit is applied to prevent erosion in the pipeline.

After the velocity of the fluid is known, then the Reynold number (Re) can be calculated:

$$\mathrm{Re} = \left(\frac{\rho\, v\, ID}{\mu}\right) \tag{2}$$

In accordance with the Reynold number, there are two types of flow; laminar and turbulent. In laminar flow, viscous forces are dominant as it is characterized by a smooth, constant, fluid motion, while turbulent flow occurs at high Reynolds numbers and is dominated by inertial forces.

Furthermore, the friction factor can be calculated based on the type of flow, whether it is laminar or turbulent. The value of Re is to determine the friction factor (f) is as follows:

$Re \leq 2500$

$$f = \left(\frac{64}{\mathrm{Re}}\right) \tag{3}$$

$Re > 5000$

$$f = \frac{0.25}{\left(log_{10}\left[\frac{\frac{\varepsilon}{ID}}{3.7} + \frac{5.74}{Re^{0.9}}\right]\right)^2} \tag{4}$$

Equation 4 is the *Swamee–Jain* equation used to solve directly for the *Darcy–Weisbach* friction factor f for a full-flowing circular pipe. It is an approximation of the implicit Colebrook–White equation.

Then the friction head (H_f) is calculated by:

$$H_f = \frac{f\, v^2 L_e}{2\, g\, ID} \tag{5}$$

where L_e is length equivalent:

$$L_e = L_p + n_b h_{eq} ID + n_v h_{eq} ID + n_r h_{eq} ID \tag{6}$$

Pressure drop due to friction along the pipe can be expressed by:

$$\Delta P_f = \rho\, g\, H_f \tag{7}$$

To calculate the pressure drop due to elevation difference can be done by using:

$$\Delta P_H = \rho\, g\, (z_e - z_s) \tag{8}$$

Therefore, the total pressure drop in the single-phase flow is:

$$\Delta P_t = \Delta P_f + \Delta P_H \tag{9}$$

3.2 Two-phase flow

The Ulubelu geothermal field is a typical water-dominated system. For such a system, the fluid flow from the well is a two-phase flow, consisting of steam and water. An average steam fraction of 20% means that the percentage of steam is only 20% of the total two-phase flow. The two-phase flow pattern

in the pipeline will vary depending on many factors, such as the pipe orientation (horizontal or vertical), pipe diameter, fluid flow rate, liquid or gas phase, pressure, temperature, etc. The classification of the two-phase flow pattern will be divided into two. First, the two-phase flow in a vertical pipe that can be found in the flow from the reservoir where the fluid flashes in the wellbore until the two phases are discharged from the well. Secondly, the two-phase flow in a horizontal pipe, flowing from wellhead to separator. Since this study is about the SAGS, then the basic theory of two-phase flow pattern in a horizontal pipe will be explained. In a horizontal pipe, the determination of the flow pattern is based on the ratio of the superficial velocity of gas and liquid. Several types of flow are experienced in a horizontal pipe, as can be seen in Figure 6 (Baker, 1954).

1. Bubble flow: steam bubbles form and flow in the top of the pipe at a velocity approximately equal to the velocity of the liquid phase.
2. Plug flow: fluid plug and steam bubbles alternately move at the top of the pipe.
3. Stratified flow: the liquid phase flows at the bottom of the pipe while the steam phase flows over it. The boundary between the liquid and steam phases is called the steam-liquid interface.
4. Wavy flow: similar to stratified flow, liquid phase flows at the bottom while the steam phase flows over it, but because the steam phase moves faster, then the steam-liquid phase interface becomes wavy.
5. Slug flow: the steam phase flowing at a higher velocity than the liquid converts the flow into slug flow.
6. Annular flow: liquid phase in the form of layers flows along the pipe wall and steam in the centre of the pipe at high velocity.
7. Dispersed (mist flow): Occurs when a continuous steam phase with liquid granulates dispersed throughout the steam. This is commonly referred to as fog flow or mist flow.

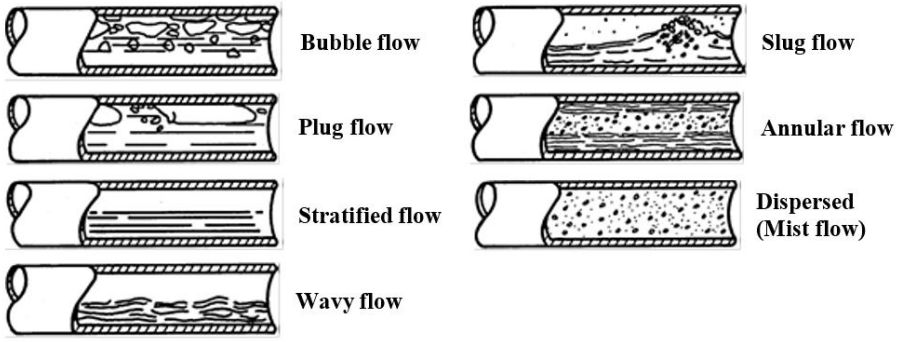

FIGURE 6: Two-phase flow types in a horizontal pipe (Baker, 1954)

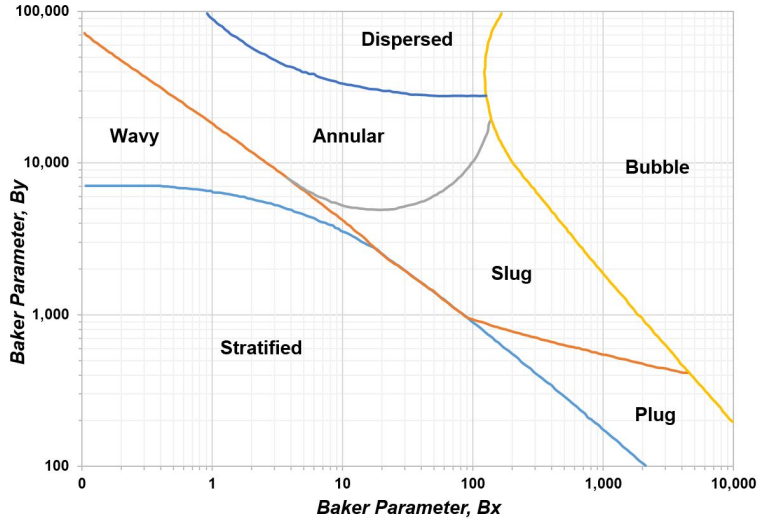

FIGURE 7: Baker map to predict two-phase flow regime (Baker, 1954)

The relationship between superficial gas and liquid velocities with flow patterns is illustrated in a flow pattern map. The flow pattern map can be used to predict two-phase flow patterns inside the pipeline. Several flow pattern maps have been published, including the Baker map (Baker, 1954), (Figure 7), Hoogendorn map (Hoogendorn, 1959), Mandhane map (Mandhane et. al., 1974), Mukherjee and Brill map (Spedding and Watterson, 1998), Spedding and Nguyen map (Spedding and Watterson, 1998), Lin and Hanratty map (Spedding and Spence, 1993), and the

Universal flow regime map (Spedding et. al., 2003). In principle, all the flow pattern maps are a prediction so it cannot be determined exactly which one is the most accurate. In this study, Baker's and Mandhane's maps will be used to determine flow patterns in two-phase pipes. The Baker map determines the two-phase fluid pattern as shown in Figure 7.

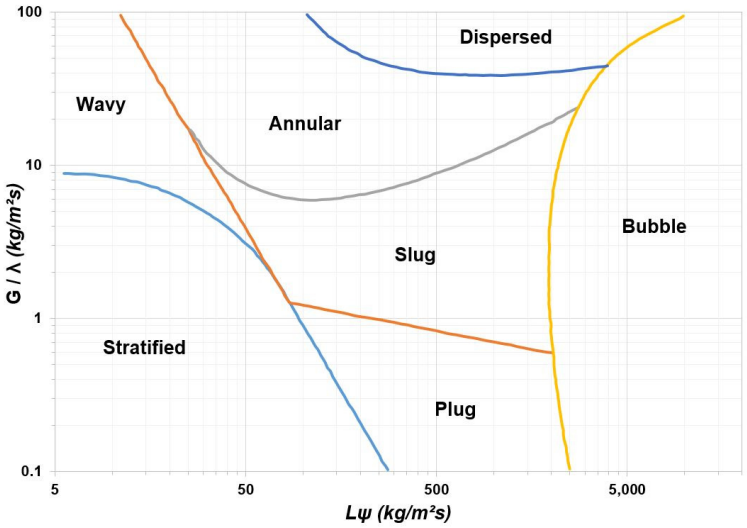

FIGURE 8: Modified Baker's map for horizontal flow (Whalley, 1987)

The Baker map, which was published in 1954, determines the two-phase flow pattern by plotting the Baker parameters, B_x on the x-axis and B_y in the y-axis. The Baker map for horizontal pipe is a logarithmical graphic, and with it the Baker parameters can be defined as:

$$B_x = 531\left(\frac{1-x}{\mathrm{x}}\right)\left(\frac{\rho_v^{0.5}}{\rho_L^{0.167}}\right)\left(\frac{\mu_L^{0.333}}{\sigma_L}\right) \tag{10}$$

and

$$B_y = 2.16\frac{Q\ x}{A(\rho_L\rho_v)^{0.5}} \tag{11}$$

Whalley, 1987 modified and improved Baker's map and published a new modified two-phase flow pattern map as shown in Figure 8. He changed the dimensionless units of Baker map to SI units.

From the Figures 7 and 8, G and L are the mass fluxes of the gas and liquid phases, respectively. The equation to calculate the parameters ψ and λ are:

$$\psi = \left(\frac{0.0724}{\sigma_L}\right)\left(\frac{\mu_L}{0.0009}\left(\frac{1000}{\rho_L}\right)^2\right)^{1/3} \tag{12}$$

and

$$\lambda = \left(\frac{\rho_G}{1.2}.\frac{\rho_L}{1000}\right)^{1/2} \tag{13}$$

To assess the two-phase flow pattern determination, Mandhane et al. (1974) can be used. It gives a good approach since in their experiment they used a large amount of experimental data (the AGA-API two-phase flow data bank) from research between 1962 and 1973. They took all the results of horizontal flow and based on that defined their own map (Figure 9).

The superficial fluid velocities, G and L for gas and liquid, respectively, are determined based on the volumetric gas flow Q_{VS} and volumetric liquid flow Q_L as follows:

$$V_{SG} = \frac{Q_{VS}}{A} \tag{14}$$

and

$$V_{SL} = \frac{Q_L}{A} \tag{15}$$

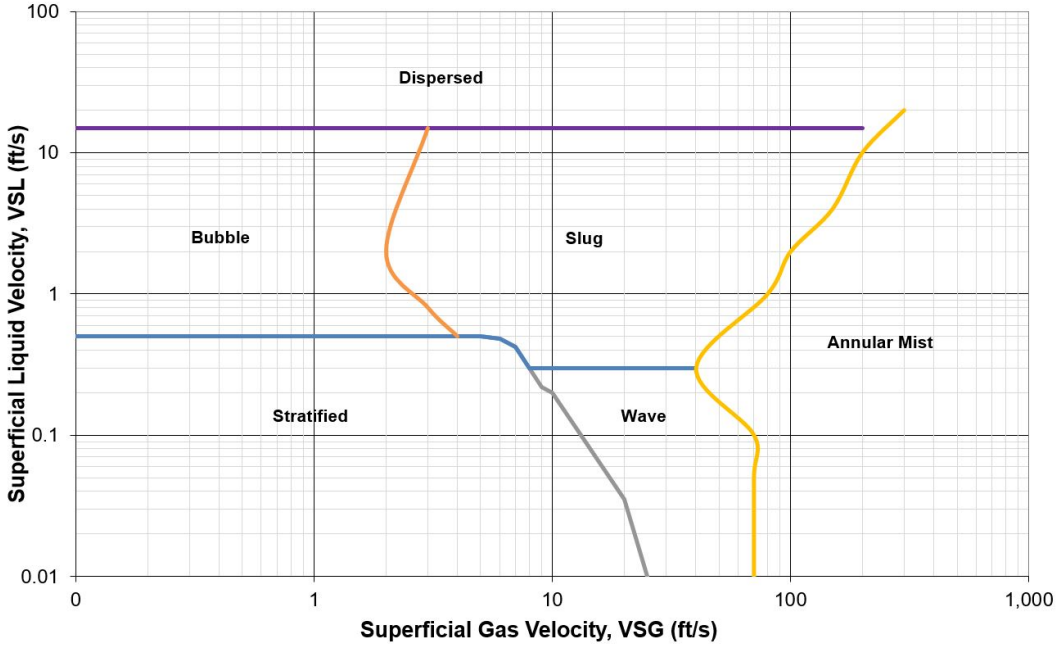

FIGURE 9: Two-phase flow pattern map by Mandhane et al. (1974)

The calculations for two-phase flow are more complex than for single-phase flow. It is also very difficult to derive an equation to obtain two-phase fluid properties. Therefore, two-phase fluid properties are often obtained empirically.

In this study, the calculation of the pressure drop in the two-phase fluid uses a separated flow model, where the void fraction (α) is an important parameter. Void fraction is the ratio of the steam flow cross-section (A_g) to the total cross-section (A):

$$\alpha = \left(\frac{A_g}{A}\right) \tag{16}$$

Zhao et al., 2000 modified and improved the pressure drop equation in the two-phase fluid pipeline of Harrison (Bergthórsson, 2006) by explaining the correlation of a new void fraction derived from a two-phase velocity distribution analysis using the Seventh Power Law. This equation is then used in the calculation of pressure drop due to length:

$$\frac{1-\alpha}{\alpha^{7/8}} = \left[\left(\frac{1}{x}-1\right)\left(\frac{\rho_G}{\rho_L}\right)\left(\frac{\mu_L}{\mu_G}\right)\right]^{7/8} \tag{17}$$

To predict the pressure drop in a two-phase flow, it is assumed that an equivalent pseudo single-phase flow has the same boundary layer velocity distribution. The average velocity of it is used to determine the wall friction factor. The velocity also has good parameter correlation to predict pressure drop in two-phase flow in the horizontal pipe.

The void fraction determines other two-phase flow parameters, such as the average liquid phase velocity (V_f) and average density (ρ). Zhao et al. (2000) explain that the average liquid phase velocity can be calculated using the following equation:

$$\bar{V}_f = 1.1\,(1-x)\,\frac{\dot{m}\,(1-x)}{\rho_l\,(1-\alpha)\,A} \tag{18}$$

In Equation 18, 1.1(1-x) is used as correction factor mainly for the entrainment. This correction factor is selected to give a good result rather than having a rigorous theoretical justification. The average velocity of the equivalent single-phase flow ($\bar{V}$) is calculated as:

$$\frac{\bar{V}_f}{\bar{V}} = \frac{\left(1 - \sqrt{\alpha}\right)^{8/7} . \left(1 + \frac{8}{7}\sqrt{\alpha}\right)}{(1 - \alpha)} \tag{19}$$

By using the Reynolds number and the friction factor in Equations 2 and 4, the pressure drop due to length is calculated as (Zhao et. al., 2000):

$$\Delta P_L = \frac{f\, \rho_L\, \bar{V}^2}{2\, ID_{pipe}\, (1 - AC)} . L \tag{20}$$

where:

$$\mathrm{AC} = \frac{m_g}{\rho_G\, P\, A^2 \alpha} \tag{21}$$

If two-phase fluid flows through an installation such as a bend, expansion unit (reducer), valve etc., then the flow pattern will be disrupted. However, it is more difficult to create a two-phase flow model across a bend than a single-phase flow because the two-phase flow is very complex and is influenced by the centrifugal force. Pressure loss in the bend is influenced by various parameters and there is no analytical calculation method that can calculate those accurately. Therefore, the commonly used method multiplies the single-phase pressure losses by an empirical two-phase multiplier as is common for a straight pipe analysis. Chisholm (1983) proposed the multiplier for the liquid flowing alone:

$$\varphi^2{}_{BLO} = 1 + \left(\frac{\rho_L}{\rho_G} - 1\right)(B\, x\, (1 - x) + x^2) \tag{22}$$

and

$$B = 1 + \frac{2.2}{K_{BLO}\left(2 + \left(\frac{r}{\mathrm{ID}}\right)\right)} \tag{23}$$

Then, the pressure drop through the installation can be calculated by:

$$\Delta P_{fi} = \frac{f\, \rho_m \bar{V}^2}{2\, ID}\left(\varphi^2{}_{BLO,b}\, n_b h_b ID + \varphi^2{}_{BLO,r}\, n_r h_r ID + \varphi^2{}_{BLO,v}\, n_v h_v ID\right) \tag{24}$$

Therefore, the total pressure drop in the two-phase flows in the pipeline becomes:

$$\Delta P_t = \Delta P_L + \Delta P_{fi} + \Delta P_H \tag{25}$$

3.3 Pipe wall thickness

The thickness of the pipe for the design pressure is calculated based on following the formula from ASME 31.1. Power Piping (ASME, 1995):

$$t_n \geq t_m = \frac{P\, D_o}{2\,(S_h\, E + P\, y)} + A_{mc} \tag{26}$$

In case of the SAGS of Unit-1 and Unit-2, the operational and design condition for every class is shown in Table 3.

In this study, pipe thickness is not calculated since it is already determined in the design phase. During the operation phase, the pipe thickness is monitored along the pipeline, starting from production wells area to the steam lines and the interface area, and from the reinjection lines to reinjection wells. These measurements of thickness will be compared to give information about pipes at present condition and will predict the remaining operating life of the pipes and separators based on several classifications of action plans for future strategy.

3.4 Separator performance analysis using Lazalde-Crabtree's method

In 1984, Lazalde-Crabtree presented a paper titled "Design approach of steam water separators". In this paper, the efficiency of the separator is measured by the amount of brine water transferred from the steam and this definition has been universally accepted as a way of measuring separator efficiency. Lazalde-Crabtree also stated that the efficiency of the separator is the result of the product of the mechanical efficiency and the annular efficiency. Figure 10 shows the main dimensions of the vertical Webre-cyclone separator in Ulubelu.

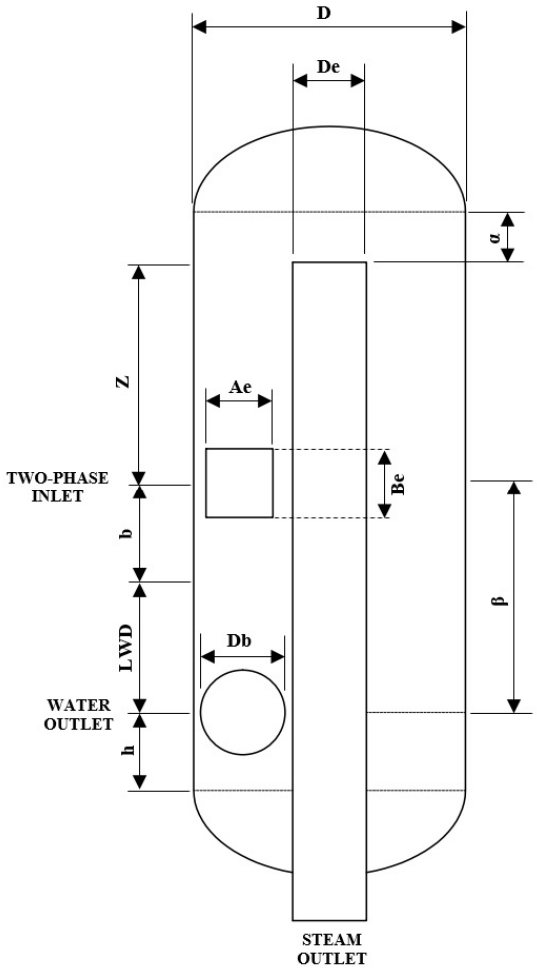

Dimension of separator:
Ae = inlet mixture width (m)
Be = inlet mixture length (m)
D = diameter of separator (inside) is 2.52 (m)
Db = diameter of water outlet (m)
De = diameter of steam outlet (m)
D_T = estimated diameter (m); Determined by Q_{VS} and assuming the initial V_T value.
D_t = standard diameter, used as reference in the calculation of main dimension (m); It is an adjustment between the estimation dimension of D_T and the standard diameter of the pipe on the market. D_t = 30 inch.
LWD = the length of the integral water drum (m)
α = defined by figure 6 (m)
β = defined by figure 6 (m)
Z = defined by figure 6 (m)

FIGURE 10: Main dimensions of the vertical Webre-cyclone separator (PGE, 2006)

The efficiency of the separator is the mass ratio of separated liquid to inlet liquid. To calculate the efficiency of the separator, Lazalde-Crabtree uses this equation:

$$\eta_{ef} = \eta_M \times \eta_A \tag{27}$$

Leith and Licht (1972) provide an approach to calculate the centrifugal efficiency. Higher centrifugal efficiency will be achieved when the steam inlet velocity increases:

$$\eta_M = 1 - \text{EXP}\left[-2\,(\psi C)^{\frac{1}{2n+2}}\right] \tag{28}$$

$$\frac{1-n_1}{1-n} = \left(\frac{294.3}{T+273.2}\right)^{0.3} \tag{29}$$

$$n_1 = 0.6689\ D^{\,0.14} \tag{30}$$

$$\psi = \frac{\rho_w \, d_w^2 \, (n+1)u}{18 \, \mu_V \, D} \tag{31}$$

$$\mathrm{u} = \frac{Q_{VS}}{A_O} \tag{32}$$

The parameter C is a cyclone design number, reflecting the physical shape of the cyclone:

$$\mathrm{C} = \frac{8 \, K_C D^2}{A_O} \tag{33}$$

For separator: $$A_O = A_e B_e \tag{34}$$

For dryer: $$A_O = \frac{\pi (D_T)^2}{4} \tag{35}$$

where $$K_C = \frac{t_r \, Q_{VS}}{D^3} \tag{36}$$

$$t_r = t_{mi} + \frac{t_{ma}}{2} \tag{37}$$

$$t_{mi} = \frac{vo_s}{Q_{VS}} \tag{38}$$

$$vo_s = \frac{\pi}{4}(D^2 - D_e^2)z \tag{39}$$

$$t_{ma} = \frac{vo_H}{Q_{VS}} \tag{40}$$

$$vo_H \cong vo_1 + vo_2 - vo_3 \tag{41}$$

$$vo_1 = \frac{\pi D^2}{4}\alpha \tag{42}$$

By assuming ASME flange and dished head:

$$vo_2 = 0.081 \, D^3 \tag{43}$$

$$vo_3 = \frac{\pi D_e^2}{4}(\alpha + 0.169D) \tag{44}$$

From Equation 28, it can be seen that the centrifugal inertial impaction parameter (Ψ) is sensitive to d_w, therefore an accurate estimate of d_w is needed to get an accurate result for Ψ. Lazalde-Crabtree modified the equation of Nukiyama and Tanasawa (1938), by adding terms in the following way. This way, d_w can be calculated as below:

$$d_w = \frac{A}{v_T^a}\sqrt{\frac{\sigma_L}{\rho_L} + BK\left[\frac{\mu_L^2}{\sigma_L \rho_L}\right]^b \left(\frac{Q_L}{Q_{VS}}\right)^c v_T^e} \tag{45}$$

where A = 66.2898; K = 1357.35; b = 0.2250; and c = 0.5507.

$$v_T = \frac{4Q_{VS}}{\pi D_T^2} \tag{46}$$

The variables of a, B and e are dependent on the type of two-phase flow pattern determined using Baker's method (Lawrence, 1952) and are given in Table 6.

TABLE 6: Variables a, B and e to be used in Equation 45

Type of two-phase flow pattern	a	B	e
Stratified or wavy	0.5436	$94.9042\ (X_s)^{(-0.4538)}$	0.0253
Annular	0.8069	$198.7749\ (X_s)^{(0.2628)}$	-0.2188
Dispersed or bubble	0.8069	$140.8345\ (X_s)^{(0.5747)}$	-0.2188
Plug or slug	0.5436	$37.3618\ (X_s)^{(-6.88x10-5)}$	0.0253

The entrainment efficiency (η_A) defines the entrainment and increases significantly with high velocities and can be calculated using Equation 47 below. The entrainment efficiency increases when upward annular steam velocity (v_{AN}) goes down:

$$\eta_A = 10^j \tag{47}$$

$$\mathrm{j} = -3.384(10^{-14})(v_{AN})^{13.9241} \tag{48}$$

$$v_{AN} = \frac{4Q_{VS}}{\pi(D^2 - D_e^2)} \tag{49}$$

$$0 \leq \eta_A \leq 1 \tag{50}$$

$$\mathrm{x}_i = \frac{h_M - h_L}{h_v - h_L} \tag{51}$$

Table 7 shows the recommended parameters to be considered in the design of the separator and dryer.

TABLE 7: The recommended parameters in separator and dryer design (Lazalde-Crabtree, 1984)

Parameter	Separator	Dryer
Max steam velocity at inlet mixture pipe	45 m/s (150 fps)	60 m/s (195 fps)
Recommended steam velocity at inlet mixture pipe	25-40 m/s (80-130 fps)	35-50 m/s (115-160 fps)
Max annular upward steam velocity inside cyclone	4.5 m/s (14.5 fps)	6.0 m/s (20 fps)
Recommended annular upward steam velocity inside cyclone	2.5-4.0 m/s (8-13 fps)	1.2-4.0 m/s (4-13 fps)
$R_1 = D/D_T$	3.3	3.5
$R_2 = D_e/D_T$	1	1
$R_3 = D_b/D_T$	1	*
$R_4 = \alpha/D_T$	-0.15 **	-0.15 **
$R_5 = \beta/D_T$	3.5	3
$R_6 = z/D_T$	5.5	4

*) Should be calculated as a drain

**) This ratio is negative because of the nomenclature (inside the head)

Lawrence (1952), Ludwing (1977) and Shepperd and Lapple (1939) explained the equation to calculate the gas pressure drop in the separator as follows:

$$\Delta P_{sep} = \frac{(NH)\ u^2\ \rho_v}{2} \tag{52}$$

where

for separator:

$$\mathrm{NH} = 16\left(\frac{A_e B_e}{D^2}\right) \tag{53}$$

and for dryer:

$$\mathrm{NH} = 16\left(\frac{\pi D_T^2}{4\,D_e^2}\right) \tag{54}$$

When the efficiency of the separator has been calculated, the outlet steam quality can be determined, as the mass ratio of outlet steam to outlet steam-water. This can be expressed as:

$$x_o = \frac{W_V/W_L}{1 - \eta_{ef} + W_V/W_L} \tag{55}$$

3.5 Silica Saturation Index - SSI

Silica Saturation Index (SSI) is a method used as a first step in the process of determining the potential of silica scaling in a well. The SSI value is determined by the solubility of silica in the fluid. Some of the factors that determine the solubility of silica include temperature, salinity and pH. In general, the higher temperature, the greater silica solubility (Fournier and Rowe, 1977). This is because of the greater energy available to break the bonds between molecules in the dissolution process. Figure 11 shows the solubility of quartz and amorphous silica at various temperatures. The relationship of silica solubility to temperature among others can be expressed by the Fournier equation (Equation 56).

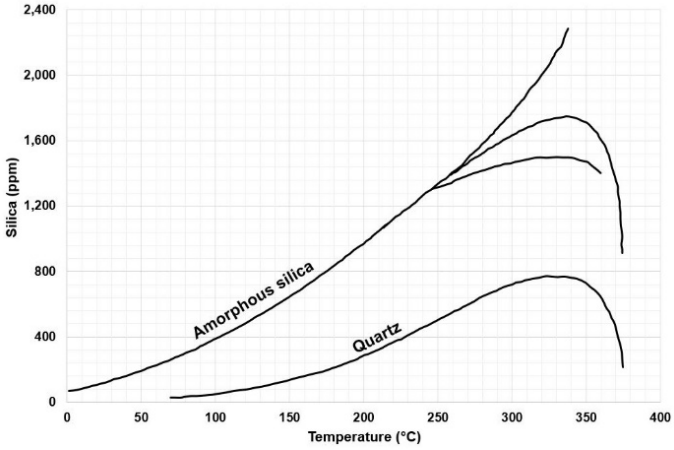

FIGURE 11: The solubility of quartz and amorphous silica at various temperatures (Fournier and Rowe, 1977)

Hamrouni and Dhahbi (2001) explained that salinity shows the salt content in the fluid. Some studies show that greater salinity will decrease the silica solubility. The correction of silica solubility in saline solutions can be expressed by the Setschenow, Chen and Marshall equations (Equations 57-59). Figure 12 shows the solubility of silica in the presence of several types of salts in the fluid.

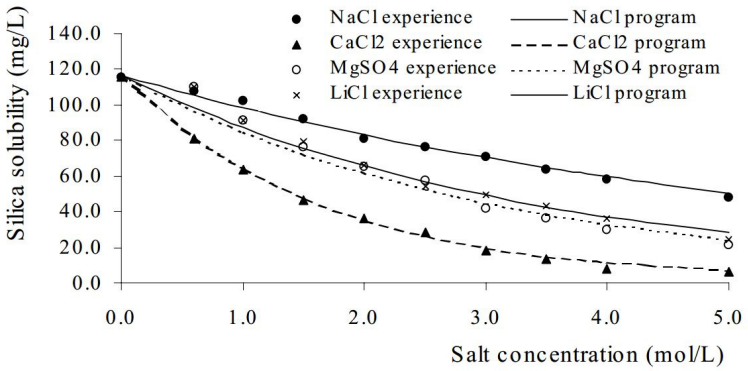

FIGURE 12: Predicted and determined silica solubility vs salt concentration (Hamrouni and Dhahbi, 2001)

SSI can be determined by comparing the measured silica concentrations at the production facility with the theoretical silica solubility. The SSI value is a thermodynamic quantity that determines the possibility of silica scaling. If the SSI < 1, then the silica in the fluid is in undersaturated state, and tends not to cause scaling, but if SSI > 1, then silica is supersaturated and tends to cause scaling. If SSI = 1 then the silica in the fluid is in an equilibrium state. The SSI can be calculated using the following steps:

1. Calculate the theoretical solubility of amorphous silica in water using the Fournier equation:

$$\log s_0 = 4.52 - \left(\frac{731}{T}\right) \tag{56}$$

2. Correct the silica solubility in the presence of fluid salinity based on the equations of Setschenow, Chen and Marshall:

$$\log D = -1.0569 - 1.573 * 10^{-3} t \tag{57}$$

$$m_{cl} = \frac{[Cl^-]}{35.5 * 1000} \tag{58}$$

$$s_{sat} = s_0 * 10^{-mD} \tag{59}$$

3. Calculate SSI by:

$$\text{SSI} = \frac{SiO_{2\ brine}}{s_{sat}} \tag{60}$$

3.6 Stodola's cone law or Law of the Ellipse

Cooke (1983) explained how to model off-design, multi-stage turbine pressure by using Stodola's ellipse. He also explained that during the design phase of the power plant, an owner or the engineer should request to the manufacturer to explore off-design and/or abnormal conditions between or beyond the normal load points. In a geothermal power plant, due to decline of production wells when makeup wells have not been drilled, it most likely occurs. Then the power plant will operate at off-design or under off-design of normal condition. Operating pressure, temperature and steam flow to the power plant will decrease and the outcomes, which is power generation, will decrease too. In this period, to maintain the performance of power plant and to ensure the safe operation of it, information about the limit of operation of the power plant must be available.

Stodola's cone law or Law of the Ellipse is a method to provide the nonlinear correlation of chamber pressure against steam mass flow inlet of the turbine. It is very useful in turbine off-design calculations. The off-design steam flow inlet is $\dot{m}_{01}$, the pressure and temperature inlet, respectively, are P_{01} and T_{01}, while outlet pressure is expressed by P_{21}.

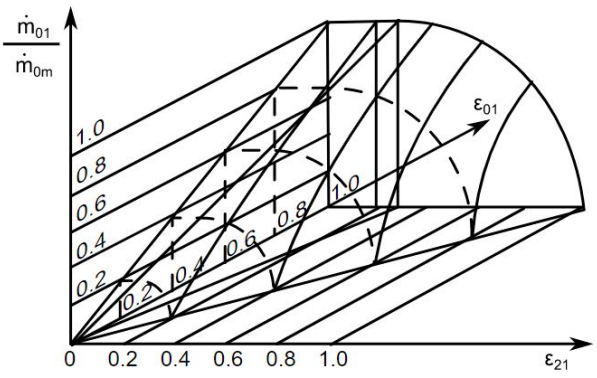

FIGURE 13: Prediction of chamber pressure using Stodola's cone law (Wikipedia, 2017)

The geothermal power plant type is mostly a condensing type with very low or vacuum turbine outlet pressure. At this condition, the turbine outlet pressure is constant so the inlet steam mass flow does not change (Figure 13). The steam mass flow will change depending on inlet pressure. For the condensing unit, the steam mass flow ratio is defined as (Wikipedia, 2017):

$$\frac{\dot{m}_0}{\dot{m}_{01}} = \frac{\epsilon_0}{\epsilon_{01}} = \frac{p_0}{p_{01}} \tag{61}$$

where ϵ_0 and ϵ_{01} respectively are the pressure ratios for the design and off-design conditions and m is at maximum condition:

Hence:

$$\epsilon_0 = \frac{p_0}{p_{0m}} \tag{62}$$

$$\epsilon_{01} = \frac{p_{01}}{p_{0m1}} \tag{63}$$

4. THE ASSESSMENT RESULT

4.1 Steam availability at present condition

After five years of operation from 2012 to 2017, the steam availability for the SAGS Unit-1 and Unit-2 has decreased significantly due to a decline in production wells. The production wells in Ulubelu are declining every year, both in terms of pressure and production capacity. Figure 14 below shows the phenomenon, where the pressure data and total flow are taken from the tracer flow test (TFT) results from 2012 to 2016.

The average decline of well head pressure (WHP) and total flow annually in Ulubelu is 7% (PGE, 2017b) with the highest decline of production wells in Cluster-D and the lowest in Cluster-B. In some cases, e.g. UBL-12, due to pressure decline, when the power plant has rejection load then the back pressure to the well causes the well to not produce. This is because the WHP has reached the maximum discharge pressure, so for a non-artesian well then the well will not produce. This phenomenon is characterised by the pressure in the two-phase line being higher than WHP. This well has to be disconnected several times from the SAGS and blown to a flash tank to raise and stabilize the WHP before it can be connected to the SAGS again. In case of well UBL-07 in Cluster-C, the total flow declined significantly from 2015 to 2016 due to a production casing problem, and in the middle of 2016, the 13-$^{3}/_{8}$" production casing was replaced with 9-$^{5}/_{8}$" casing. In addition, wells UBL-07, UBL-06 and UBL-12 also had a similar problem, with their production casing also replaced with a smaller diameter casing.

For well UBL-16 in Cluster-B, the total flow decline is quite significant compared to other wells in the same Cluster. In accordance with Figure 14a, in 2013, the WHP increased due to the setting of the throttle valve in the two-phase line after the wellhead where the valve opening at that time was subtracted from the previous opening to keep the wells in and joining another well in the header.

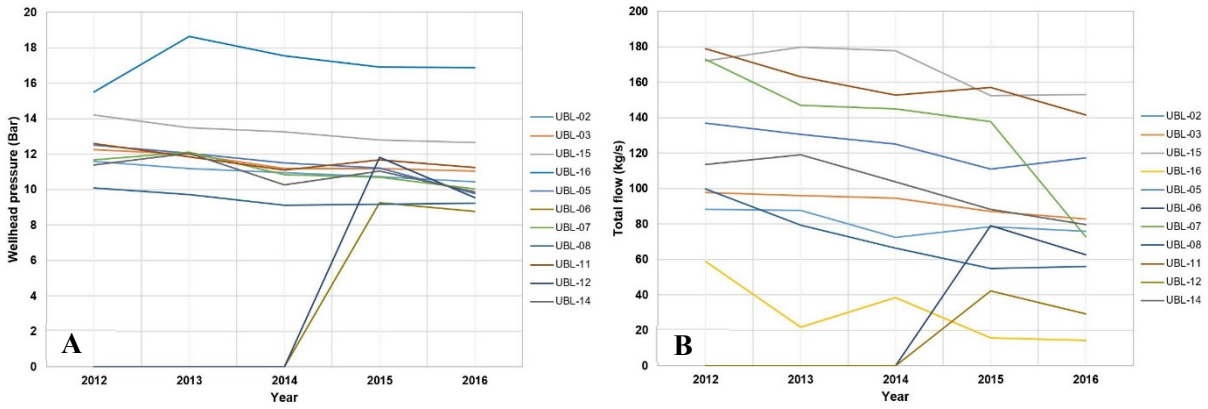

FIGURE 14: Wellhead pressure (a) and total flow (b) of production wells of Unit-1 and Unit-2, Ulubelu from 2012 to 2016

Steam availability of Unit-1 and Unit-2 based on the TFT at the end 2016 (PGE, 2017b) is displayed in Table 8. It shows that at present conditions, the enthalpy and dryness of production wells in Ulubelu have decreased compared to initial operations in 2012, which are represented by the design condition. The exploration and exploitation department of PGE explains that there is an indication of a temperature drop in the reservoir due to the close connection between production wells and reinjection wells. This statement is supported by tracer results in 2014. They recommend that reinjection wells should be moved to a further location. New reinjection wells have therefore been drilled in the middle of 2016, which are located close to the reinjection wells for Unit-3 and Unit-4. By the end of 2017, it is planned that the reinjection from Cluster-A will have been moved to the new reinjection wells. However, new locations for the reinjection wells for Cluster-F are not available due to land acquisition problems for pipelines.

TABLE 8: Steam availability of Unit-1 and Unit-2, Ulubelu at the end of 2016

Well	Design conditions							Present condition (by TFT)						
	WHP (bar-a)	% NCG	Steam (kg/s)	Brine (kg/s)	Total (kg/s)	Enthalpy (kJ/kg)	X (%)	WHP (bar-a)	% NCG	Steam (kg/s)	Brine (kg/s)	Total (kg/s)	Enthalpy (kJ/kg)	X (%)
CLUSTER-B														
UBL-2 (B1)	11.75	1.76	18.46	61.40	79.86	1253.60	23.12	11.11	0.40	14.00	61.80	75.80	1128.37	18.47
UBL-3 (B2)	11.75	1.16	20.76	63.57	84.33	1283.90	24.62	11.50	1.40	15.40	67.30	82.70	1126.78	18.62
UBL-15 (B4)	11.79	0.61	29.68	92.05	121.72	1280.10	24.38	13.91	1.04	32.00	121.10	153.10	1201.74	20.90
UBL-16 (B5)	11.79	1.90	19.23	64.10	83.33	1253.50	23.08	18.92	3.08	3.70	10.60	14.30	1361.19	25.87
Sub total / average		**1.26**	**88.14**	**281.11**	**369.25**	**1267.78**	**23.8**		**1.10**	**65.10**	**260.80**	**325.90**	**1204.52**	**20.97**
CLUSTER-C														
UBL-5 (C1)	10.31	0.54	12.62	79.04	91.67	1045.70	13.77	9.44	0.21	15.40	101.80	117.20	993.30	13.14
UBL-6 (C2)	10.33	0.36	16.12	81.10	97.22	1102.50	16.58	10.89	0.16	8.70	54.10	62.80	1047.24	13.85
UBL-7 (C3)	10.33	0.38	20.77	104.51	125.28	1102.50	16.58	10.71	0.20	10.90	61.70	72.60	1024.29	15.01
UBL-8 (C4)	10.3	0.44	15.07	76.60	91.67	1099.20	16.44	10.44	0.17	7.30	48.70	56.00	1025.47	13.04
Sub total / average		**0.42**	**64.58**	**341.25**	**405.83**	**1087.48**	**15.84**		**0.19**	**42.30**	**266.30**	**308.60**	**1022.58**	**13.76**
CLUSTER-D														
UBL-11 (D1)	12.90	0.56	42.08	139.06	181.14	1271.80	23.23	11.29	0.40	27.00	115.40	142.40	1141.92	18.96
UBL-12 (D2)	12.90	1.23	13.76	50.79	64.56	1233.60	21.32	10.10	0.98	6.70	22.50	29.20	1212.66	22.95
UBL-14 (D4)	12.90	0.55	24.43	74.12	98.56	1302.60	24.79	9.77	0.40	15.70	64.00	79.70	1145.62	19.70
Sub total / average		**0.67**	**80.27**	**263.98**	**344.25**	**1269.33**	**23.11**		**0.48**	**49.40**	**201.90**	**251.30**	**1166.73**	**20.53**
Total / average		**0.83**	**232.99**	**886.34**	**1119.33**	**1208.19**	**20.92**		**0.66**	**156.80**	**729.00**	**885.80**	**1131.27**	**18.42**

4.2 Heat mass balance at present conditions

Due to changes of operating parameters such as pressure, temperature, enthalpy and total flow in production wells, it is necessary to monitor the SAGS performance. One of the monitoring tools is the heat mass balance (HMB), which is the known condition of operating parameters on each stream number as shown in the process flow diagram in Figure 4. The HMB in Table 2 is the design condition, so that needs to be updated with data at present condition. The HMB calculation was done using Engineering Equation Solver - EES (F-Chart Software, 2017), and to simplify the calculation the SAGS was divided into several sections. The first section is the two-phase line from each Cluster, i.e. Cluster-B, C and D to the separator. The second section is the steam line, from the separator to the interface point and the third section is the brine line, from the separator to the reinjection wells in Cluster-A and F. The calculation flowchart of the pressure drop in the two-phase line is shown in Appendix I, while a summary of operating parameters on each stream number is shown in Table 9.

In the HMB simulation seen in Table 9, it is shown that the decline of operating parameters in the production wells, especially pressure and total flow, causes decreasing parameters in the steam line, especially at the interface point. At the design condition, the interface point pressure that PGE must meet to supply steam to PLN as the owner of the power plant is 8 bar-a, while from the above simulation the interface pressure calculated at the present condition is 7.62 bar-a. This will affect turbine operation, so that the turbines will operate at the off-design condition.

However, before concluding the statement above, it is necessary to validate the simulation results using the EES with the actual parameter measurement results in the field. The measurement of operation parameters in the field was done by a pressure transmitter, which can be monitored in the central control room. Table 10 below displays the comparison between simulation results and actual measurements in the field.

Bergthórsson, 2006 explains that the average acceptable error of calculation in two-phase flow compared with the actual measurement results in the field using the field instrument is 36-52% (roughness dependent models). From Table 10, it can be seen that about 67% of the simulations of the pressure drop

TABLE 9: Heat mass balance of the SAGS Unit-1 and Unit-2 Ulubelu at present condition

Stream number		1	2	3	4	5	6	7	8	9	10
Fluid properties	Units	CLUSTER-B				CLUSTER-C				CLUSTER-D	
		2 ϕ from UBL-02	2 ϕ from UBL-03	2 ϕ from UBL-15	2 ϕ from UBL-16	2 ϕ from UBL-08	2 ϕ from UBL-05	2 ϕ from UBL-06	2 ϕ from UBL-07	2 ϕ from UBL-12	2 ϕ from UBL-11
Pressure	bar-a	11.11	11.50	13.91	18.92	9.51	9.44	10.89	10.71	10.10	11.29
Temperature	°C	184.50	186.10	194.80	209.60	177.70	177.40	183.70	182.90	180.30	185.30
Mass flow	Ton/h	272.88	298.08	550.44	51.48	201.60	421.92	225.72	261.36	105.12	418.32
	kg/s	75.80	82.80	152.90	14.30	56.00	117.20	62.70	72.60	29.20	116.20
Enthalpy	kJ/kg	1128.37	1126.78	1201.74	1361.19	1025.47	993.30	1047.24	1024.29	1213.00	1142.00
Steam fraction	%	17.27	16.89	19.02	24.47	13.46	11.93	13.38	12.38	22.25	17.81
Stream number		11	12	13	14	15	16	17	18	19	20
Fluid properties	Units	CLUSTER-D									
		2 ϕ from UBL-14	2 ϕ from Cluster-B	2 ϕ from Cluster-C	2 ϕ from Cluster-D	2 ϕ Cluster-B	2 ϕ Cluster-C	Steam at Cluster-B	Steam at Cluster-C	Steam at Cluster-D	Steam
Pressure	bar-a	9.77	10.75	8.70	9.19	9.96	8.57	7.91	8.39	8.29	7.85
Temperature	°C	178.90	183.10	174.00	176.30	179.70	173.30	170.00	172.40	171.90	169.60
Mass flow	Ton/h	286.92	325.80	308.50	810.36	325.80	308.50	237.24	151.92	172.08	280.62
	kg/s	79.70	90.50	85.69	225.10	90.50	85.69	65.90	42.20	47.80	77.95
Enthalpy	kJ/kg	1146.00	1172.62	1017.40	1152.00	1172.62	1017.40	2767.82	2770.21	2769.75	2768.10
Steam fraction	%	19.18	19.55	13.35	19.72	19.55	13.38	100.00	100.00	100.00	100.00
Stream number		21	22	23	24	25	26	27	28	29	30
Fluid properties	Units	Steam	Steam	Steam	Steam to GPP	Hot Brine to Cluster-A	Hot Brine to Cluster-A	Hot Brine to Cluster-F	Hot Brine at Cluster-A	Hot Brine at Cluster-F	Condensate to Cluster-A
Pressure	bar-a	7.65	7.83	7.63	7.62	7.91	8.39	8.29	12.49	16.34	14.30
Temperature	°C	168.60	169.50	168.50	168.40	169.90	172.40	171.90	168.60	170.50	50.00
Mass flow	Ton/h	47.8	280.62	77.95	561.24	933.48	925.92	722.16	1859.40	722.16	290.40
	kg/s	13.28	77.95	21.65	155.90	259.30	257.20	200.60	516.50	200.60	80.67
Enthalpy	kJ/kg	2767.04	2768.04	2766.93	2766.87	718.90	729.60	727.50	713.40	721.60	209.30
Steam fraction	%	100.00	100.00	100.00	100.00	0.00	0.00	0.00	0.00	0.00	0.00

TABLE 10: Comparison result of simulation by EES and measurement by field instrument

No.	Section	Line	Measurement by field instrument			Simulation by EES			Error (%)
			P_0 (bar-a)	ΔP (bar/m)	P_1 (bara)	P_0 (bara)	ΔP (bar/m)	P_1 (bara)	
1	Two phase	- Header Cl-B to Sep-01A	9.84	0.001237	8.15	10.75	0.000577	9.96	53.31
		- Header Cl-C to Sep-01B	9.44	0.015663	8.48	8.70	0.002233	8.57	85.74
		- Header Cl-D to Sep-02	8.58	0.002085	8.42	9.19	0.002655	8.99	27.34
2	Steam	- Cl-C to Header at interface point	7.72	0.000058	7.68	7.85	0.000035	7.83	40.37
		- Cl-D to Header at interface point	8.11	0.000176	7.50	8.29	0.000191	7.63	8.67
		- Header to Interface point	7.50	0.000130	7.49	7.63	0.000139	7.62	7.09
3	Brine	- Cl-C to Cl-A	7.72	-0.000351	8.65	7.87	-0.001730	12.49	393.38
		- Cl-D to Cl-F	8.11	-0.003558	15.83	8.29	-0.003709	16.34	4.25

Note: P_0 at design condition and P_1 at present condition.

is within this range but one result above the range. Generally, these conditions can be caused by several factors. From the calculation side the equation used was obtained from the experimental results in pipes with a maximum diameter of 4" (Bergthórsson, 2006), while the actual SAGS pipes in Ulubelu diameter vary from 12 to 52". From the actual data, the measurement is the more accurate result considering the detailed configuration of the pipe, while the calculation is an approximation, which gives not exactly the same conditions as in the field. An example is the large error that occurs in the measurement of pressure drop in the brine line from Cluster-C to Cluster-A. The assumption in the simulation only considers the input condition and output point, whereas the actual configuration is not always downhill, there are several lines of pipes that go up and down. Also, errors from field instruments cannot be ruled out. Before the measurement is carried out it must be ensured that all measuring equipment has been calibrated. However, the results of the simulation calculations using EES software are still acceptable.

In addition, we can compare the two-phase flow pattern between the design conditions and the present condition. The simulation of the two-phase flow pattern using EES can be seen in Appendix II. Figure 15 below shows the comparison of the flow pattern between the two conditions. The comparison is made using the modified Baker by Whalley, 1987 (subscript 1) and confirmed by another method in Mandhane et al. 1974 (subscript 2) where (a) is the design condition and (b) is the present condition. Based on both methods, both design and present conditions show basically the same result, in which the majority have an annular flow pattern type. The difference in outcomes between the design and present conditions above is due to changes in operating parameters such as pressure, enthalpy, dryness and two-phase flow from the wells.

The flow pattern type will be proportional to the two-phase flow rate in the pipeline following a logarithmic scale. On the x-axis, for design conditions, the pressure, dryness and two-phase flow are greater than at the present condition and as a result, the superficial steam velocity is also greater. This is displayed in the flow pattern plot, which for the same stream number at the present condition on the x-axis, shifts to the left. On the y-axis, it can be observed that the flow pattern plot in Ulubelu at present conditions, slightly shifts downward. This is also due to the decline in operating parameters of pressure, enthalpy, dryness and two-phase flow.

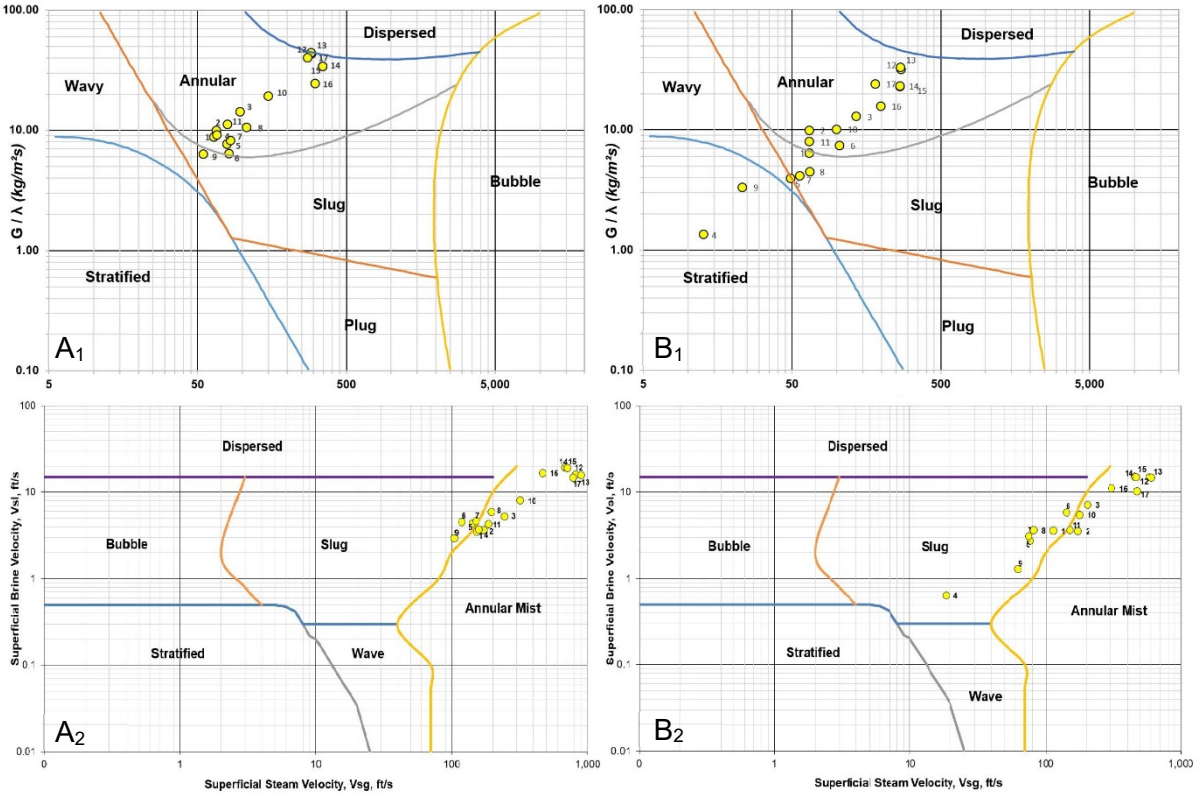

FIGURE 15: Two-phase flow pattern of Unit-1 and Unit-2, Ulubelu at design condition (a) and actual condition (b). Modified Baker's flow pattern by Whalley, 1987 (subscript 1) and by Mandhane et. al., 1974 (subscript 2)

In fact, the annular or dispersed type is the flow pattern that is commonly encountered for two-phase flow in pipes. This flow pattern is also a desirable flow pattern type because the two-phase flow in the pipe is divided into two, where high-density water is along the wall of the pipe while the low-density vapour is in the centre of the pipe. However, in Figure 15 there is a change in the flow pattern of the two-phase flow in the pipe for streams number 4, 5, 6, 7 and 8 from annular to slug/stratified. Those stream numbers are the two-phase flows from the wellhead to the headers in each cluster, respectively, from well UBL-16 in Cluster-B and wells UBL-08, 05, 06 and 07 in Cluster-C.

Theoretically, the slug flow occurs because the vapour is moving faster than the water and causes a collision in the pipe, which is characterized by the vibrations in the pipe that occur intermittently. At actual conditions in the field, since the two-phase line from the well to the header in each cluster does not have a large diameter with a short distance, this does not cause significant problems. If slug flow occurs in large diameter pipes with long distances, for example in the two-phase pipeline from Cluster-B to Cluster-C, then that should be the main concern. However, from the flow pattern map (Figure 15) it is shown that the flow pattern of two-phase flow from Cluster-B to Cluster-C is annular flow type; it is still the same as the design conditions (shown in streams number 12 and 13).

In terms of fluid velocity in the pipeline, especially the two-phase pipeline from the header to separator, the steam pipeline from the separator to the interface point and the brine pipeline from the separator to the reinjection wells, the decrease of the total flow rate from the well will also reduce the fluid velocity in the pipeline. The maximum recommended fluid velocity in the pipeline for two-phase flow is equal to its erosion velocity (API RP 14E, 1991), whereas in the steam pipeline its maximum is 40 m/s (saturated vapour) and in the brine pipeline the maximum is 3 m/s (IPS, 1996). The comparison of fluid velocity between design and present conditions is shown in Table 11. Generally, it can be said that the fluid velocity in the SAGS of Unit-1 and Unit-2 is still below the recommended maximum velocity.

TABLE 11: The comparison of fluid velocity in pipeline at design and present condition

No	Line service	Recommended maximum fluid velocity (m/s)	Design condition (m/s)	Present condition (m/s)	Remarks
1	**Two phase**				
	- Cl-B to Sep-01A	27.16	22.65	16.33	OK
	- Cl-C to Sep-01B	23.10	19.54	13.52	OK
	- Cl-D to Sep-02	26.20	19.71	12.38	OK
2	**Steam (saturated)**				
	- Cl-C to inter. point	40.00	37.29	30.60	OK
	- Cl-D to inter. point	40.00	30.04	25.62	OK
3	**Brine**				
	- Cl-C to Cl-A	3.00	1.83	1.52	OK
	- Cl-D to Cl-F	3.00	2.54	1.90	OK

4.3 Wall thickness monitoring and evaluation

The wall thickness measurements in the SAGS Unit-1 and Unit-2 are performed on average twice a year using an ultrasonic thickness meter (Table 12). This is done with the aim of obtaining actual data on

TABLE 12: The classification of action on level of priority of wall thickness monitoring

Level of priority	Action	Remarks
1	Programme replacement immediately or derate line to suit the maximum expected current operating conditions.	Remaining wall thickness less than design minimum requirement. Requires immediate replacement or line to be derated.
2	Programme replacement in less than a year and requires close monitoring.	Corrosion rate too high. To be verified and closely monitored. Replacement to be done within one year or line derated to safe design condition if wall thickness falls below original design parameters.
3	Programme replacement in 1-5 years, requires regular monitoring.	High corrosion rate - requires regular monitoring.
4	Programme replacement in 5-10 years.	Requires regular monitoring.
5	Expected life before failure is beyond 10 years.	No significant metal loss noted, monitor as required.

wall thickness after some period of operation, and then the data is compared with the forecast of the wall thickness reduction in the same period by considering the corrosion allowance. Based on the comparison, the actual condition of the pipe during the latest measurement can be evaluated, and if there is a reduction in thickness beyond the initial conditions specified in the design phase, follow-up action can be taken immediately. The classification of follow-up action is divided into several levels depending on the last wall thickness data. In accordance with the standard AS/NZS 3788-2006 (AS/NZS, 2006) and Cruz (2014) for similar cases, the action priority is divided into several levels as shown in Table 12 below. The determination of the level of priority is done by calculating the corrosion rate or actual erosion in the pipe or separator from the last measurement data and subtracting the initial measurement data, divided by the time difference between the points. Then the result is used as a reference to predict the remaining time until the wall thickness reaches minimum thickness, which was calculated in the design phase.

The results of wall thickness measurements in SAGS of Unit-1 and Unit-2 Ulubelu are identified according to the schematic diagram below. Measurements were made on two-phase lines in each cluster, from cluster to separator and in the separator itself (Figure 16), the steam line from the separator to the interface point (Figure 17), and brine line from the separator to reinjection wells (Figure 18). The total

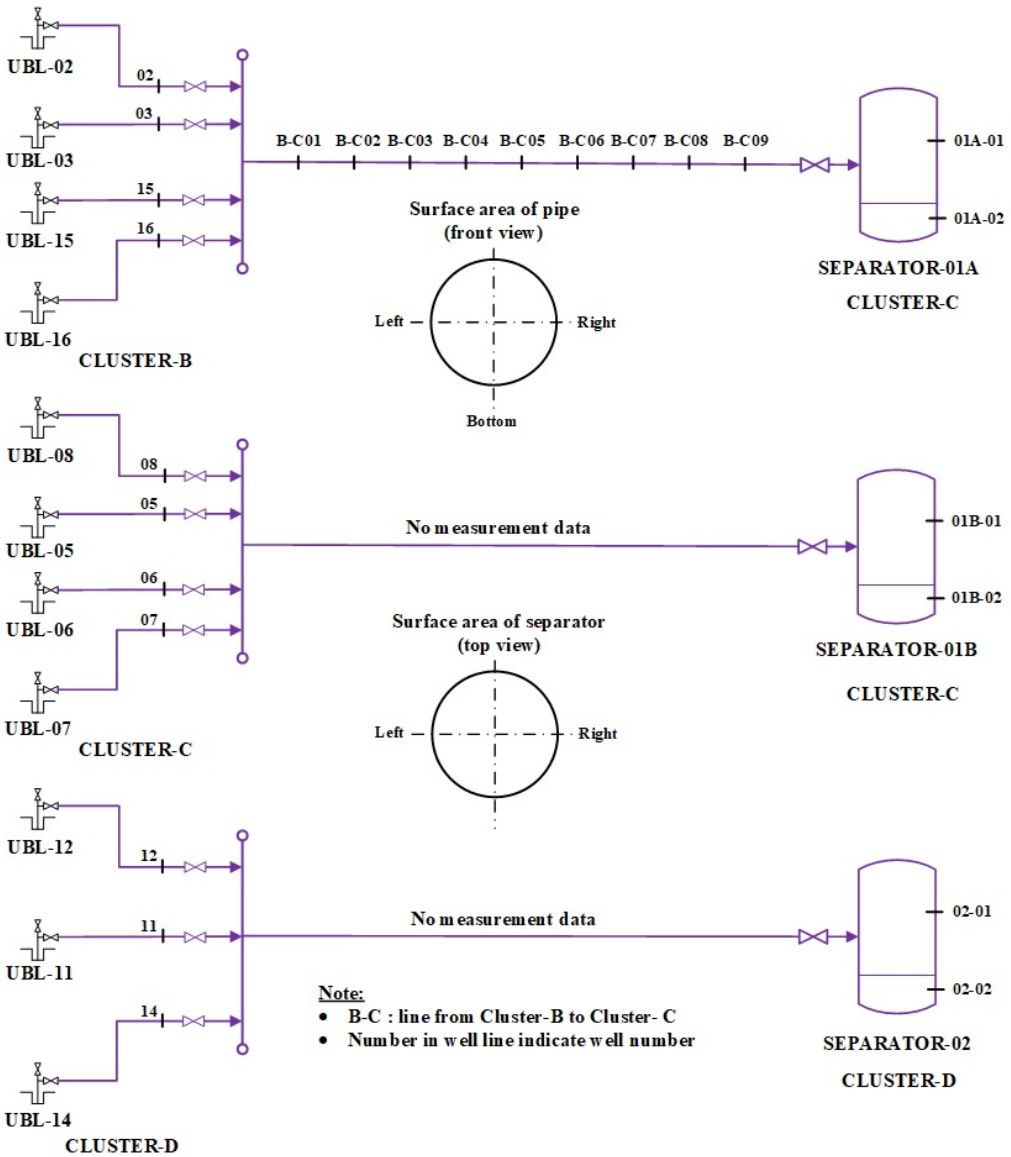

FIGURE 16: A schematic diagram of wall thickness measurement locations in the two-phase line and separators

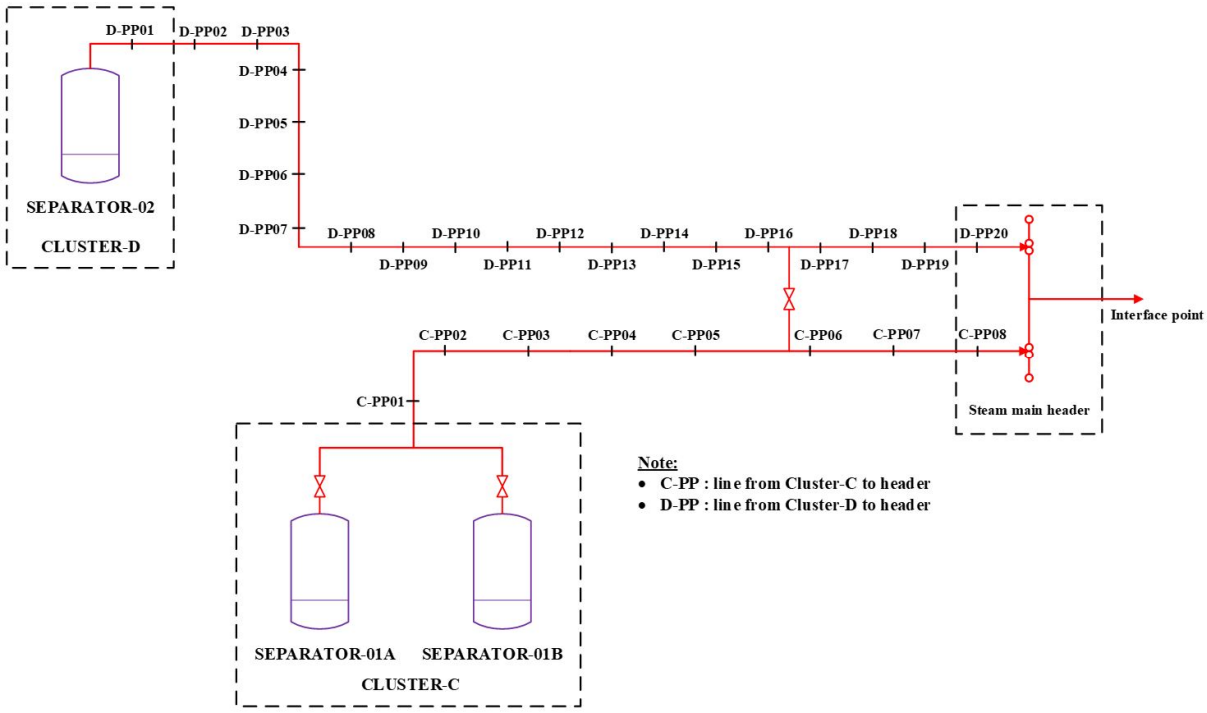

FIGURE 17: A schematic diagram of wall thickness measurement locations in the steam line from separators to header in interface area

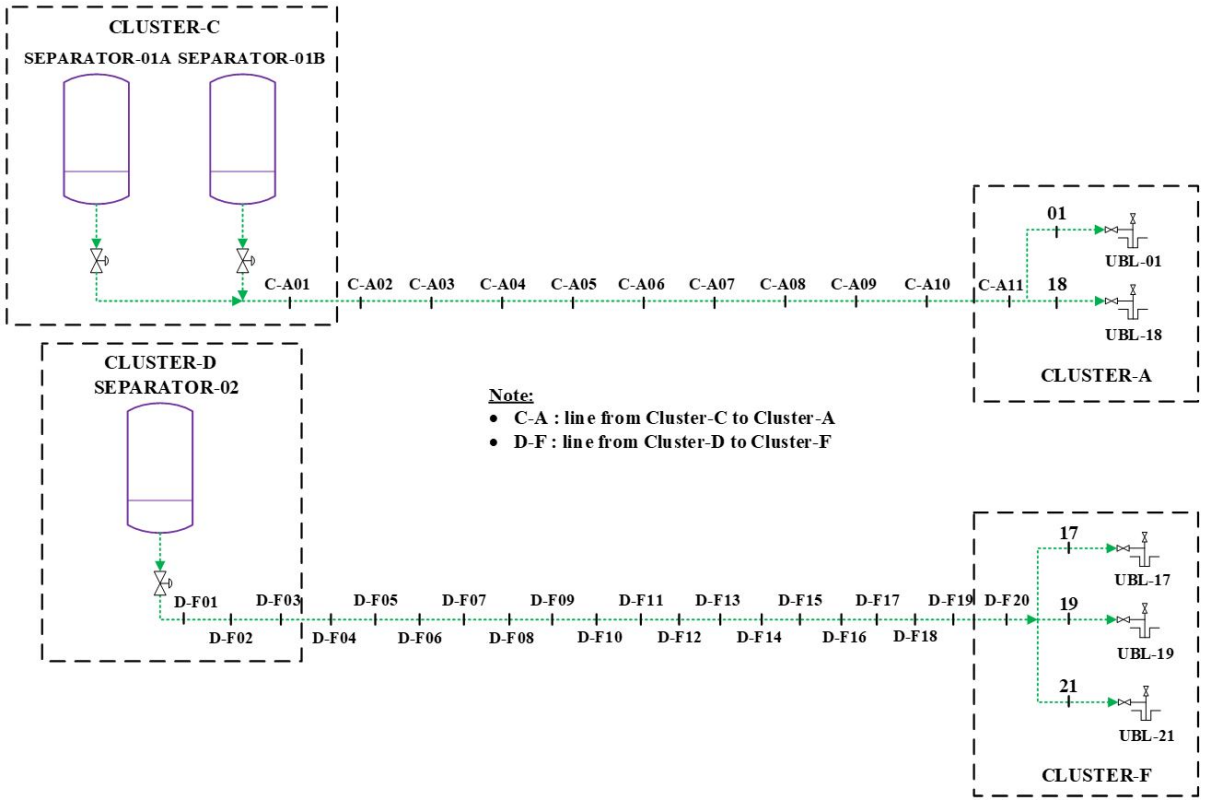

FIGURE 18: A schematic diagram of wall thickness measurement locations in the brine line from separators to reinjection well clusters

points of wall thickness measurements in the two-phase line are 26. Those consist of one point in the two-phase line in each well, nine points along the two-phase line from a header in Cluster-B to inlet Separator-01A in Cluster-C and two points in each separator, whereas there is no measurement data for the two-phase line from the header to the separator in Cluster-C and D. In the steam line, there are 28 points of measurement, which consists of eight points in the steam line from Cluster-C to the interface point and 20 points from Cluster-D to the interface point. In the third section. There are 36 points of measurement in the brine line from the separator to the reinjection well clusters. These consist of 11 points from Cluster-C to Cluster-A, 20 points from Cluster-D to Cluster-F and five points in each well. The points of measurement are determined by dividing the pipe length into equal intervals where measurements are done.

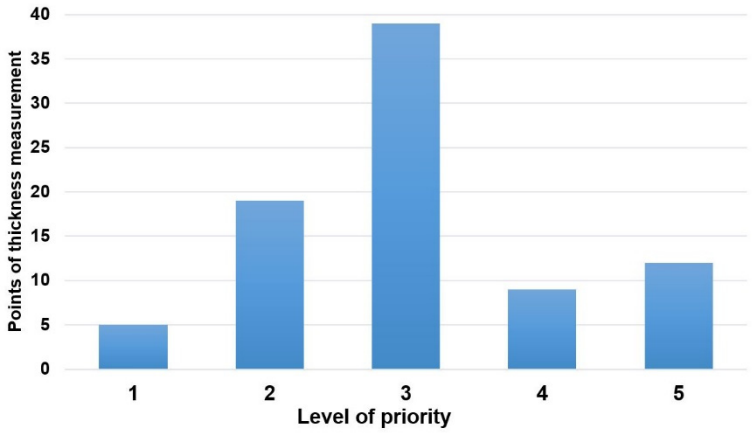

FIGURE 19: The classification of wall thickness results according to level of priority

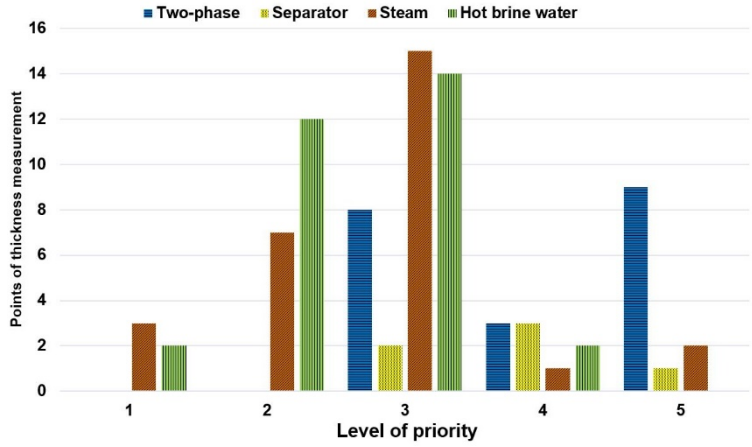

FIGURE 20: The classification of wall thickness results according to level of priority in service line

The results of wall thickness measurements in the SAGS of Unit-1 and Unit-2 have been classified based on the level of priority and action plans which must be done are shown in Appendix III. In the table in Appendix III the points are grouped after each level of priority as shown in Figure 19, while Figure 20 shows the number of points on each level of priority according to its service line.

From a total of 84 measurement points conducted from 2013 to early 2017 at the SAGS of Unit-1 and Unit-2, five measurement points have a priority level 1, 19 have a priority level 2, 39 have a priority level 3, 9 have a priority level 4 and 12 have a priority level 5. For the priority levels 3 to 5, the action to be taken is that the measurement of wall thickness should be done regularly following the planning program. However, for priority levels 1 and 2, immediate action is required according to Table 12 above.

At priority level 1, there are three points in the steam line, specifically the steam line from Cluster-C to the interface point – i.e. points C-PP05, 06 and 08, and there are two points in the brine line, specifically the brine line from Cluster-C to Cluster-A – i.e. points C-A01 and 02. These five points should get serious attention and immediate follow up. Also, it would be better to measure several times at these points and several points around them to ensure the accuracy of the measurements that have been made before. Likewise, for priority level 2, the measurement time range also needs to be narrowed to monitor routinely the wall thickness conditions so the action to be done can be decided on immediately.

4.4 Separator performance analysis

An analysis of the separator performance at the present conditions is necessary in order to determine whether it is still operating efficiently or not. The decline of operating parameters in the production well will cause changes the in input conditions to the separator and this needs to be evaluated so that follow-up action can be taken if the separator performance, at present condition, is lower than the design condition. In this study, the separator performance calculation was done using EES. The comparison of the results in separator performance between design and present conditions is displayed in Table 13 below.

TABLE 13: The comparison of separator performance calculation at design and present condition

Separator	Allowable		Design condition					Present condition				
	ΔP (Bar)	Wetness interface point	Flow pattern	η_{ef} (%)	x_o (%)	w_o (%)	ΔP (bar)	Flow pattern	η_{ef} (%)	x_o (%)	w_o (%)	ΔP (bar)
Separator-01A	0.47	≤ 1%	Dispersed	99.888	99.666	0.334	0.39	Dispersed	99.784	99.140	0.861	0.24
Separator-01B	0.25	≤ 1%	Dispersed	99.880	99.384	0.616	0.20	Dispersed	99.764	98.572	1.428	0.10
Separator-02	0.30	≤ 1%	Dispersed	99.916	99.724	0.276	0.24	Dispersed	99.759	98.996	1.004	0.13

To calculate the performance of the separator, one of the main influencing factors is the pattern of the two-phase flow, which goes into the separator. Lazalde-Crabtree (1984) explains that the determination of flow patterns was done using Baker's map (1954) based on the basic theory discussed earlier. The two-phase flow pattern will determine the values of a, B and e as shown in Table 6. In this study, the flow pattern type between the design and the present condition is still the same, here it is dispersed. However, as seen in Figure 21, there is a movement of the Baker parameter, especially on the especially on the y-axis (By), and it is moving downwards. This is due to a two-phase flow decline, whereas By itself is directly proportional to the two-phase flow rate. A higher two-phase flow rate will cause higher By and a lower two-phase flow rate will cause lower By.

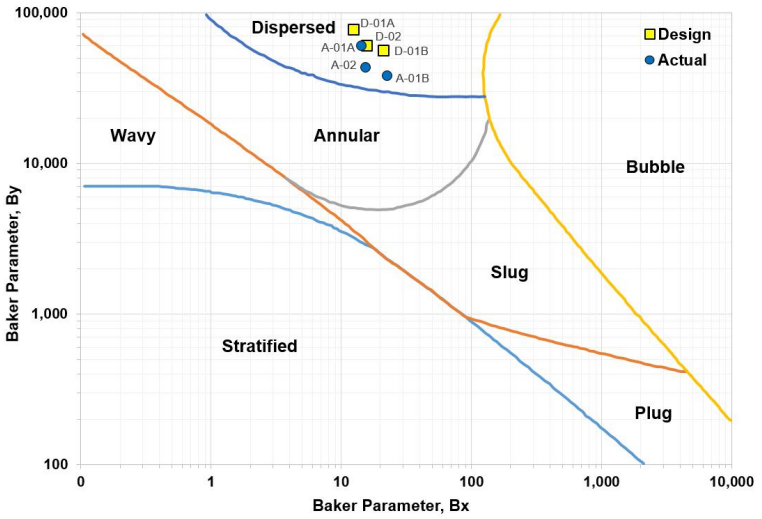

FIGURE 21: Flow pattern of two-phase flow inlet separator at Unit-1 and Unit-2, Ulubelu by Baker (1954)

The results of the separator performance calculation at the present condition are also compared with the allowable condition that must be met. Through this comparison, the performance of the separator at present conditions must meet and satisfy two requirements. First, the pressure drop in the separator should not exceed 0.47 bar in Separator-01A, 0.25 bar in Separator-01B and 0.3 bar in Separator-02. From Table 13, it is known that the pressure drop of the separator at the present condition still meets the requirements, with the calculated pressure drop as 0.24 bar in Separator-01A, 0.10 bar in Separator-01B and 0.13 bar in Separator-02. Based on these results, it can be said that the performance of the separators still meets the allowable condition.

Second is steam wetness at the interface point. According to the PJBU or steam sales contract between PGE and PLN, the steam wetness requirement in the interface point should be ≤ 1%. Although the

interface point is located quite far from the separator, it can be at least used as a reference that steam wetness outlet of separator should also be ≤ 1%. Even if the steam wetness outlet of the separator is > 1%, there is a scrubbing line along the steam line after the separator to the interface point which will dispose condensed steam along the steam pipe. This is quite helpful in minimizing steam wetness when the steam has reached the interface point. However, it is better if steam wetness can be minimized in the separation process in the separator. According to Table 13, the calculation results of wetness in the separator steam outlet at present conditions show wetness of 0.861% in Separator-01A, 1.428% in Separator-01B and 1.004% in Separator-02. Steam wetness in Separator-01A still meets the requirements, but in Separator-01B and Separator-02 the results exceed the allowable condition. However, the steam from all separators will be mixed at the main steam header in the interface point, so that the result of steam wetness that is used as a reference is at the interface point. To know the final steam wetness at the interface point, a steam condensate sample was taken from the steam line and analysed in the laboratory. From this analysis, it is known that the final steam wetness in interface point still meets the allowable conditions as shown in Table 14 below.

TABLE 14: Laboratory analysis result of steam wetness at interface point (PGE, 2017c)

No	Date	Location	Steam dryness / wetness (%)
1	March 16, 2017	Interface point	99.63 / 0.37

Although the laboratory analysis shows that steam wetness at the interface point still meets the requirements, it is necessary to optimize the performance of the separators, specifically Separator-01B and 02, to ensure that the steam wetness out of the separators meets the requirements. This is to anticipate future development, if the scrubbing line doesn‘t work optimally and the results of steam wetness at the interface point will exceed the requirements. It does not rule out that changes in operating parameters occurring dynamically may also cause changes in performance of the separator itself. Section 4.7 discusses the SAGS optimization scenarios, including the possibility of improving the performance of separators.

4.5 Silica saturation index in the reinjection line from the separator to the reinjection wells

One of the most common problems in the reinjection line from the separator to the reinjection wells is silica deposition. The silica deposition occurs due to several conditions, but in this study, we discuss the potential of silica deposition due to the silica saturation conditions in the pipeline. These conditions can be determined by the value of the silica saturation index (SSI), which is the silica concentration value in the brine at present condition compared to its solubility in the brine based on a theoretical solution (Figure 10). The value of silica and chloride in the brine can be obtained from a laboratory analysis of a sample taken in the reinjection line. In the SAGS of Unit-1 and Unit-2, there are two reinjection lines, the one from Separator-01A and 01B in Cluster-C to the reinjection wells in Cluster-A, and the line from Separator-02 in Cluster-D to the reinjection wells in Cluster-F. Table 15 shows the results of the laboratory analysis of the silica and chloride samples in both reinjection lines in early 2017.

TABLE 15: Laboratory analysis result of silica and chloride concentration in the brine line (PGE, 2017c)

No.	Location	Laboratory analysis result			
		P (bar-a)	T (°C)	Cl^- (ppm)	SiO_2 (ppm)
1	Separator-01	7.72	168.9	1200	668
2	Separator-02	8.11	171.0	1210	759
3	Cluster-A	9.12	168.5	1118	619
4	Cluster-F	12.18	170.5	1127	704

Based on the calculation steps as in the basic theory discussed earlier, the SSI in the hot reinjection line is calculated using EES. The calculation result of SSI at present conditions is compared with design conditions. Decreasing the pressure in the separator will lower the temperature as well. This will influence the temperature of the brine in the reinjection line, leading to a decrease in temperature. The temperature drop, which affected the change of solubility of silica in the brine, can be analysed through the SSI result, to see whether SSI in the reinjection line has been at its supersaturation or not. Table 16 shows the comparison of SSI between the design and the present condition.

TABLE 16: Comparison of SSI at design and present condition

No.	Location	Design condition					Present condition				
		P (bar-a)	T (°C)	Cl^- (ppm)	SiO_2 (ppm)	SSI	P (bar-a)	T (°C)	Cl^- (ppm)	SiO_2 (ppm)	SSI
1	Separator-01	9.77	178.81	1384	716	**0.929**	7.72	168.92	1200	668	**0.912**
2	Separator-02	12.31	189.20	1373	777	**0.927**	8.11	170.98	1210	759	**1.018**
3	Cluster-A	10.47	178.36	1289	664	**0.864**	9.12	168.49	1118	619	**0.848**
4	Cluster-F	18.98	188.48	1373	777	**0.932**	12.18	170.50	1127	704	**0.948**

Generally, the SSI in the brine line, both in the separator outlet and in the reinjection well cluster is still less than 1, so silica scaling will not occur, except for the SSI in the outlet of Separator-02 in Cluster-D which is above 1, which means that silica is in supersaturated condition. This indicates that at the outlet of Separator-02 silica scaling most likely will occur if the operation parameters, especially pressure and temperature, are kept in this condition. Therefore, it is necessary to optimize the operation parameters in the separator in order to prevent silica scaling in the pipeline. Figure 22 shows the plot of the SSI at the design and the present condition that supports the above statement.

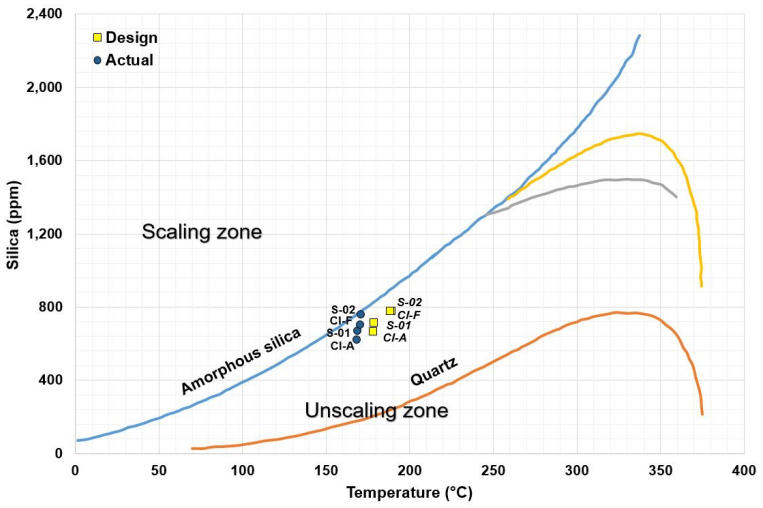

FIGURE 22: Solubility of amorphous silica at design and present condition

4.6 Turbine characteristic curve at off-design condition by Stodola's cone law

At present condition, Unit-1 and Unit-2 operate at off-design condition due to the problems described earlier. To know the effect of steam flow and pressure drop at the interface point (Table 9) on the power plant operation, a turbine characteristic curve can be used. The curve shows the relationship between the turbine chamber pressure and power generation based on steam flow rate to the power plant. The curve is provided by the turbine manufacturer for Unit-1 and Unit-2, Fuji Electric, Japan.

In this study, the author could not get the curve because the power plant is operated by PLN. Meanwhile, PGE only operates the SAGS. Therefore, Stodola's cone law was used to estimate the turbine chamber pressure and power generation based on the steam flow rate to the turbine. Some input data such as pressure, temperature and steam flow rate in some generation load conditions could be obtained through personal communication with the power plant operator. The data were measured before the main stop valve (MSV) and the main control valve (MCV), so the data did not represent the chamber pressure in

the turbine since the MCV openings greatly affected the pressure drop between them. The pressure drop on some input data above was also obtained through personal communication with the power plant operator and could be used in the calculation. Since Unit-1 and Unit-2 have the same specifications, we used data from Unit-1 as shown in Table 17.

TABLE 17: Input data from the Ulubelu power plant Unit-1
(power plant operated by PLN, personal communication, August-September 2017)

No.	P_{inlet} (bar-)	T_{inlet} (°C)	MCV open (%)	ΔP (bar)	$P_{chamber}$ (bar-g)	$\dot{m}_{steam}$ (Ton/h)	$\dot{W}_{Turbine}$ (MW)
1	6.53	167.8	90	0.19	6.34	379.82	55.55
2	6.34	166.7	68	0.28	6.06	359.86	51.88
3	5.96	164.6	42	0.73	5.23	314.45	46.59
4	6.05	165.0	30	1.71	4.34	263.52	37.85

As seen in Table 17, the data show the load generation of Unit-1 at full the load of 55 MW. According to the received information, the data were recorded when Unit-2 was going through an annual routine maintenance (minor inspection) so steam was available to maximize load generation in Unit-1.

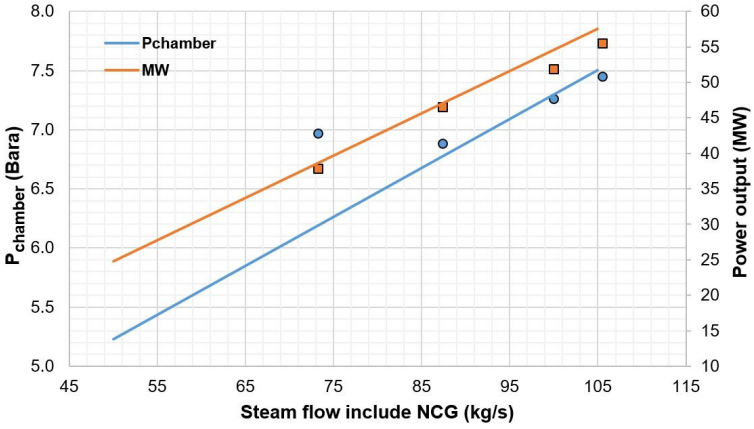

FIGURE 23: Estimation of turbine chamber pressure and power output of Unit-1 and Unit-2, Ulubelu using Stodola's cone law

Figure 23 shows the estimated turbine chamber pressure and power output of the power plant at any steam flow rate. At present condition the steam flow rate into each unit is approximately 78 kg/s which gives a prediction for a turbine chamber pressure of 6.38 bar-a and 41.5 MW of power output. This result is close to the actual conditions in which both units can only generate 42 MW power each. At this generation load, the approximate opening of the MCV before the turbine chamber is about 35% so the pressure drop between the turbine chamber with the MCV inlet is about 1.1 bar. The pressure value at inlet condition must be at least 7.53 bar-a and at the present condition, with maximum pressure in the interface point, it is 7.62 bar-a and therefore still larger than the inlet pressure of the turbine, which it should be able to hold.

4.7 Optimization scenarios

Referring to the assessment results above, the decline of operating parameters, i.e. WHP and two-phase flow in production wells, will decrease the steam pressure at the interface point. Actually, this is not a big problem as long as the steam pressure at the interface point is still above the minimum limit of 8.0 bar-a. However, at present condition, the steam pressure in the interface point drops to 7.62 bar-a, i.e. below the minimum requirement. The turbine in the power plant operates, therefore, in an off-design condition or below the operating conditions at design. In addition, the separator performance specifically related to steam outlet quality has also decreased. Some measurements of wall thickness indicate that the corrosion/erosion rate in the pipe is significant so this needs serious attention and immediate action. Monitoring the potential for silica deposition in the reinjection lines, due to the decrease in pressure and temperature in the separator, shows that the SSI in these lines is increasing, and in Separator-02 it is in

a supersaturation state. So, there is a potential of silica scaling in the reinjection line at the outlet of Separator-02. With that background, optimization scenarios are worth considering in order to improve the performance of the SAGS Unit-1 and Unit-2.

4.7.1 Varying the separator pressure

The separators are important for the SAGS because they are used to separate the two-phase flow from the production wells. The Ulubelu geothermal field has an average steam quality of only 20%, and is therefore highly dependent on separator performance. With the decrease in the separator performance indicated by the decrease in steam outlet quality, the quality of the steam delivered to the power plant will be affected. Although the final steam wetness results at the interface point still meet the required steam wetness of ≤ 1% as discussed in Section 4.4, the value will likely change according to the parameter change in the separator.

In addition, the change in separator pressure will also affect the flashing factor in the separation process of the two-phase fluid. If the two-phase flow rate entering the separator has the same flow rate and enthalpy, a higher separator pressure will decrease the value of the flashing factor and a lower separator pressure will increase the value of the flashing factor in the separator. The P-h diagram as shown in Figure 24 shows that the separation process is in the mixture area (inside the dome) and a lower separator pressure will decrease the enthalpy of saturation liquid (h_f) and the enthalpy of saturation steam (h_g). However, the reduction of enthalpy of saturation liquid is greater than the reduction of enthalpy of the saturation steam, so the flashing factor will then also increase. The result is that the steam flow rate will increase with the increase of the flashing factor because they are directly proportional to each other.

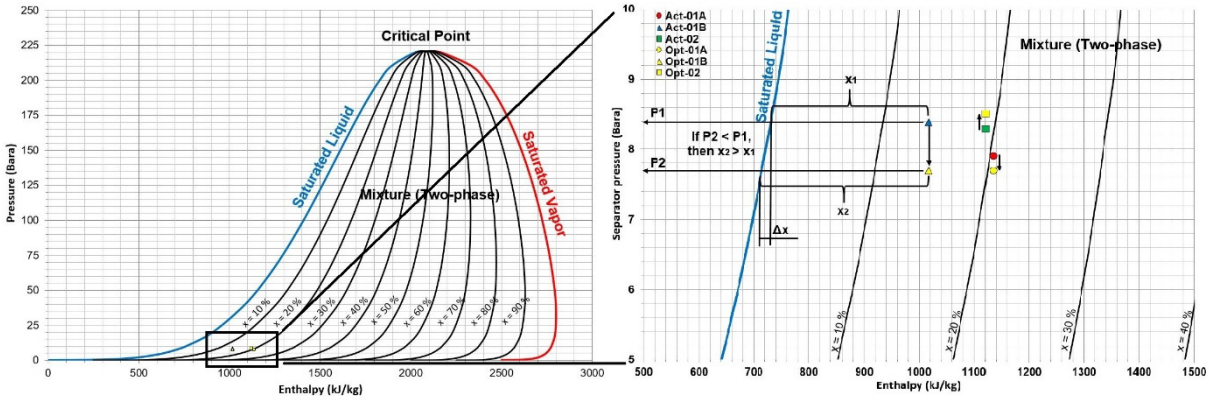

FIGURE 24: P – h diagram of water, the change of separator pressure will change the flashing factor in the separator itself

In this scenario, the separator pressure is varied to determine the separator pressure which can produce the optimum performance in terms of several aspects. First, with regard to the potential increase of the steam flow rate and, secondly, the increase of the steam outlet quality at the separator outlet. The variation of the separator pressure must also consider the pressure drop that occurs in the steam line so that the steam pressure at the interface point reaches the minimum pressure as shown in the HMB simulation in Table 9, i.e. 7.62 bar-a. Another important consideration is the prediction of the SSI value in the brine line. The SSI value in the brine line must be maintained at ≤ 1 or in the "no scaling zone". Figure 25 shows the variation of separator pressure with the increasing steam flow rate and steam outlet quality.

The target that in this scenario was to increase the steam flow rate and steam outlet quality from the separator to the interface point by considering the safe operation of the SAGS, meaning that steam outlet quality at interface point fulfils the minimum requirement of 99% and the potential of silica scaling in the brine line is minimized. Figure 25 shows the results of the performed optimization on variations of

the separator pressure. Figure 25a that by increasing the flow rate of the steam to the interface point, the present separator pressures in Separator-01A, 01B and 02 which are 7.91, 8.39 and 8.29 bar-a, respectively, are changed to 7.7, 7.7 and 8.5 bar-a, respectively. For Separators-01A and 01B, the pressure can be decreased, because according to Figure 25b SSI ≥ 1 occurs only when the separator pressure ≤ 3.8 bar-a. However, the separator pressure cannot be lowered that much, due to pressure drop in the steam line. These calculations indicate that to get the minimum pressure, 7.62 bar-a, at the interface point, the minimum separator pressure in Cluster-C must be 7.7 bar-a. Therefore, the pressure of 7.7 bar-a was selected. For Separator-02, at the present condition with pressure 8.29 bar-a the SSI value is ≥ 1. This means that the potential of silica scaling will most likely be in the brine line after the separator. Therefore, to minimize this possibility, the pressure in Separator-02 needs to be raised until SSI ≤ 1. This value will be achieved when the minimum separator pressure is 8.5 bar-a.

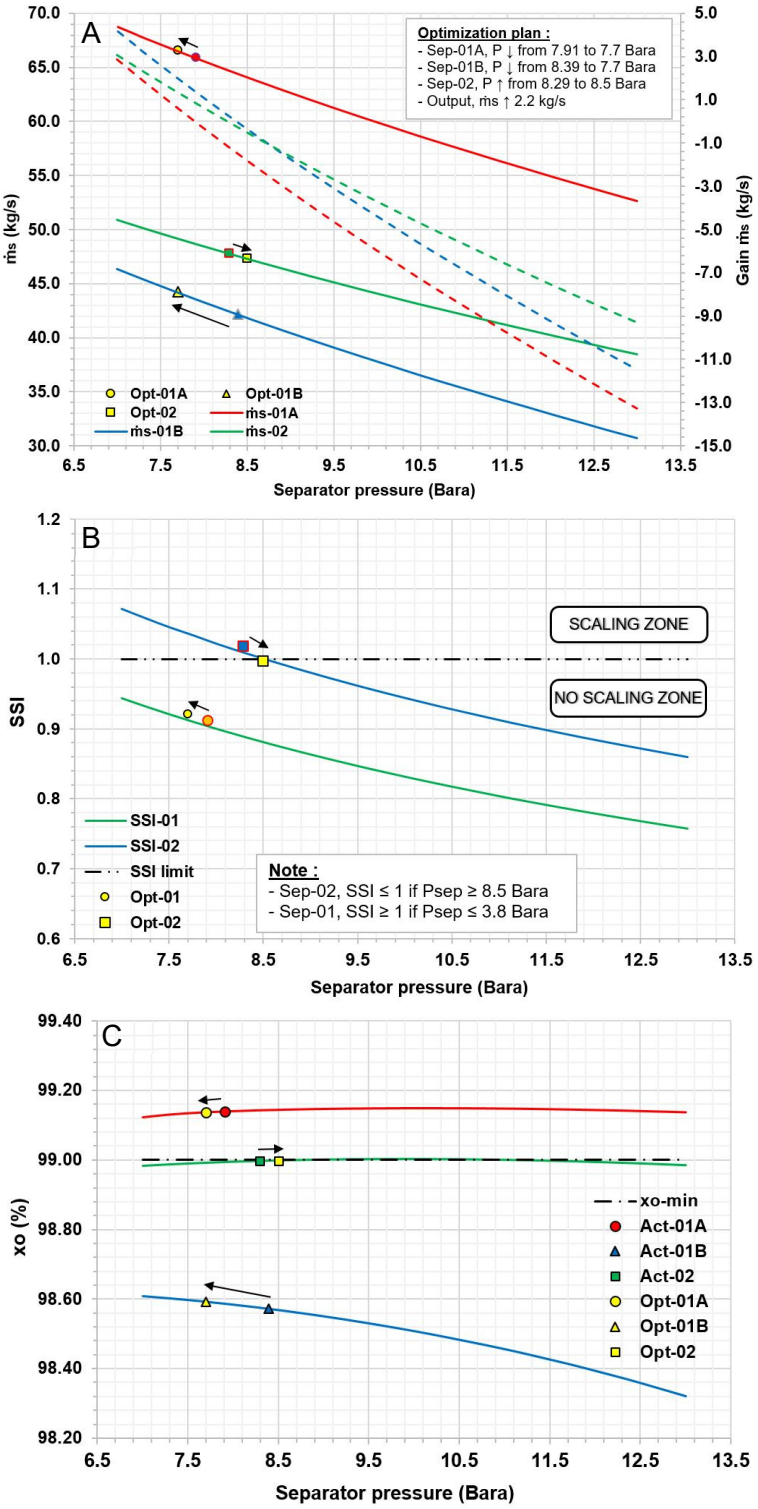

FIGURE 25: Effect of varying separator pressure on, (a) the steam flow rate; (b) SSI; and (c) steam outlet quality

The optimization result of adjusting the separator pressure has added 2.2 kg/s to the flow rate and can increase the load generation in the power plant for ~1.16 MW. Secondly, the optimization of separator pressure at some values above is seen from the steam outlet quality as shown in Figure 24c. Here, the overall steam outlet quality increases slightly, but only from 98.9027% to 98.9091%. The value is still below the minimum requirement of 99%, so from the result, it is concluded that the variation of the separator pressure is not significant in influencing the steam outlet quality in the steam line at the separator outlet. Therefore, an increase in steam outlet quality will be done with the scenario described in Subsection 4.7.2.

4.7.2 Increasing steam velocity at the separator inlet

Increasing steam velocity at the separator inlet has the purpose of increasing the outlet quality of the steam which goes to the interface point. It is stated in the steam sales contract between PGE and PLN that the minimum steam wetness at interface point should be 1%, meaning that the steam quality minimum is 99%. Even though the distance from the separators to the interface point is quite long, this requirement can be used as a basic reference for the steam quality outlet of the separators. There are two methods to increase the steam velocity at the separator inlet. First, by increasing the two-phase flow rate from the production wells. From a technical point of view, this is very easy to do by opening the valve of production wells, but practically, it is not possible since the production wells of Unit-1 and Unit-2 are already at their maximum capacity. So, the two-phase flow rate at present condition is constant, and even tends to decline with time. Therefore, the second method is more likely, which is to minimize the pipe diameter of the inlet separator. From a technical aspect, this is quite complex but still quite possible to do. Increasing the steam velocity at the separator inlet (V_T) is an effective method to increase the quality of steam at the outlet. Bangma (1961) supports this statement by explaining that the steam quality at the outlet will increase if V_T rises. The effect of V_T on the increase of separator performance is shown in Figure 26.

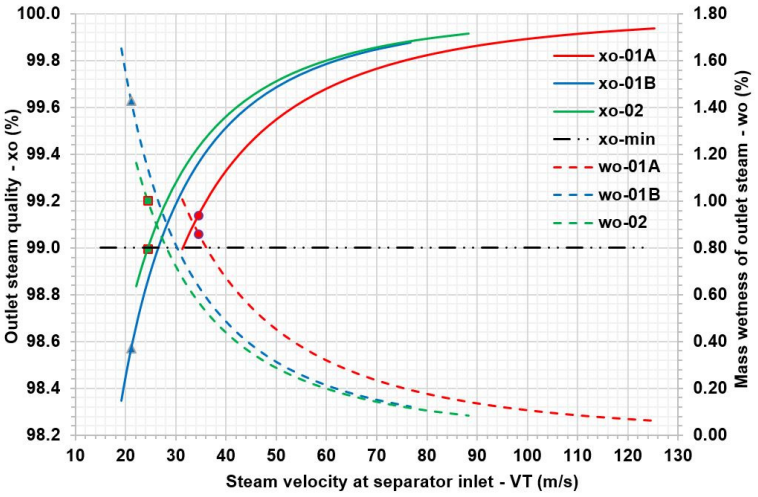

FIGURE 26: Steam quality at outlet and mass wetness of outlet steam as a function of steam velocity at the separator inlet

At the present condition, the values of the steam quality at the outlet x_o in Separators-01A, 01B and 02 are 99.14%, 98.57% and 98.99%, respectively at V_T = 34.52, 21.14 and 24.35 m/s, respectively. From Figure 25, the minimum value, which is recommended for steam quality at outlet, to be above the requirement, is the meeting point between x_o and w_o. The value for x_o for Separator-01A complies with the minimum requirement since it is already above 99% so that the steam velocity at the separator inlet value is currently at an optimum value. However, for separators-01B and 02 the values are below the requirements or less than 99%. Here it is recommended to increase the steam velocity at the separator inlet. According to the separator data, the diameter of the inlet separator is 30", and as seen in the Figure 26,V_T needs to be raised to a minimum of 28.82 m/s for Separator-01B and 26.04 m/s for Separator-02. The value of V_T in both separators will be achieved by an inlet diameter of 25.69 and 29.01", respectively. By considering availability in the market and the simplicity of installation, the selected new inlet diameter is 24". This is possible by modifying the inlet diameter of the separator, seen in Figure 27.

The example discussed above illustrates the modification for the inlet pipe of Separator-01B, where by decreasing the inlet diameter of the separator to 24", it will produce at V_T of 32.94 m/s, so the x_o rises to 99.31%. Technically, the modification is done by adding a flange connection of 36" Class 300 before a concentric reducer 30"×36", and then inside that another concentric reducer is installed of 24"×36" by welding. Then the 24" concentric reducer is connected with a 24" pipe which is 1.59 m in length. To strengthen the 24" pipe, a buffer plate 1" thick is welded on the 24" pipe and a 30" flange Class 300. This modification is quite practical because it is portable, and in the future when additional two-phase flow is available from new makeup wells, the separator inlet can be removed easily and replaced with a concentric reducer by a flange connection on both sides. However, a fluid simulation such as a 3D simulation using CFD should be used to ensure and obtain the most optimal configuration of this design before a modification is implemented.

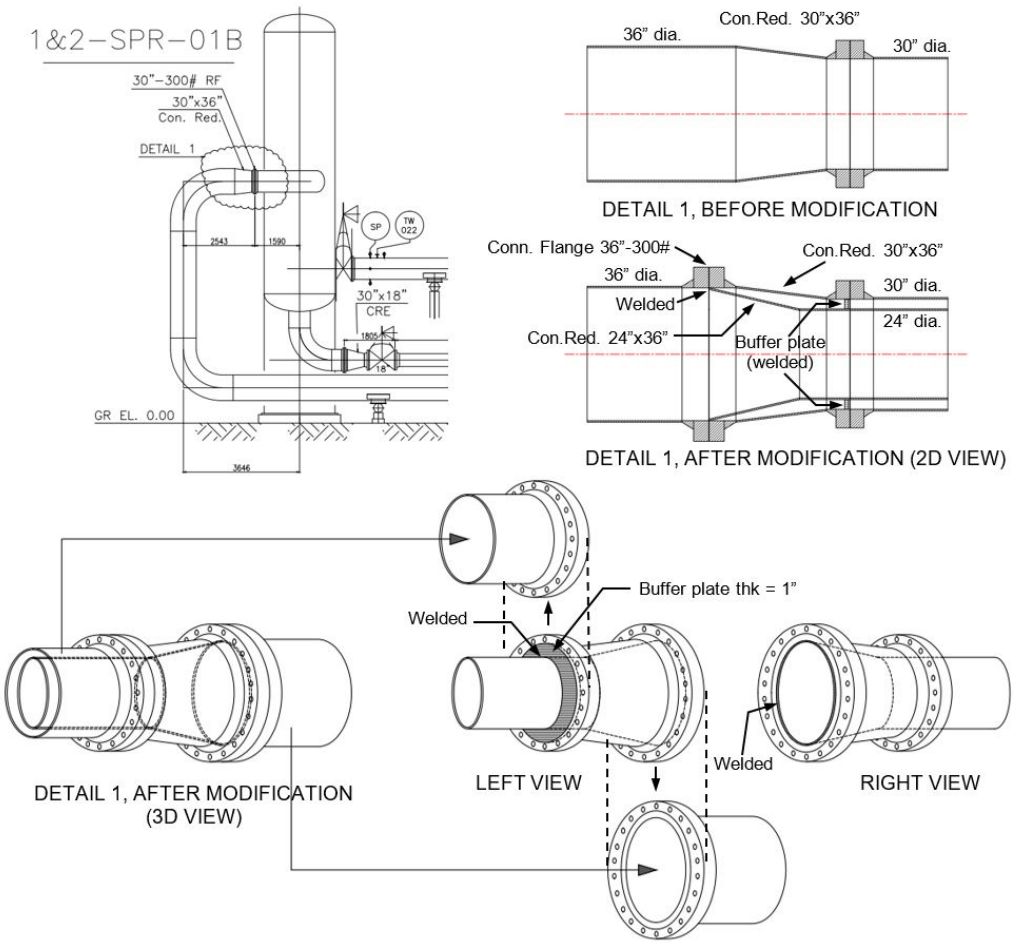

FIGURE 27: Alternative to minimize inlet diameter of separator, comparison of detail 1 before and after modification

4.7.3 Pipeline capacity mapping for future tie-in from new makeup wells or an interconnection line from Unit-3 and Unit-4 to Unit-1 and Unit-2

At the present conditions, there is a decline of the two-phase flow in the pipeline due to the decline of total flow from the production wells. Fluid velocity is proportional to the total flow, as indicated in Table 11, and the fluid velocity in the pipeline has decreased compared to the design conditions when operating at maximum load. In this case, the pipe diameter is fixed and the change of density is not significantly influential.

To find out the possibility of optimization of the pipe capacity in a future based on the present condition, it is important to map the pipe capacity in the two-phase lines. From the mapping result, recommendations can be made for some conditions that may occur. First, if a new makeup well is added close to the two-phase pipeline, the maximum flow through it can be determined. From the discharge test result of the new makeup wells, it can be decided whether it is possible to connect them to the existing pipeline or if it is necessary to build a new two-phase pipeline. Secondly, since the SAGS of Unit-1 and Unit-2 is close to Unit-3 and Unit-4, it is possible to build an interconnection line between them. Actually, at present conditions there is no excess steam supply available from the production wells of Unit-3 and Unit-4, so this interconnection line could only be used when Unit-3 or Unit-4 are under routine maintenance. In that period, steam from Unit-3 and Unit-4 can be supplied to maximize the load in Unit-1 and Unit-2. This interconnection line could also be used as an alternative to a mutual backup between the power plant and the operational flexibility of the SAGS in Ulubelu. The pipeline capacity mapping of SAGS Unit-1 and Unit-2 at present conditions is shown in Table 18.

TABLE 18: Pipeline capacity mapping of SAGS Unit-1 and Unit-2, Ulubelu at the present condition

No.	Line service	Pressure (bar-a)	Density (kg/m^3)	ID pipe (m)	Recommended maximum fluid velocity (m/s)	Maximum possible flow (kg/s)	Velocity at present condition (m/s)	Flow at present condition (kg/s)	Possibility to optimize flow in the pipes (kg/s)
1	**Two phase**								
	- Cl-B to Separator-01A	10.82	27.46	0.89	27.16	468.00	16.33	281.36	186.64
	- Cl-C to Separator-01B	8.88	32.67	0.89	23.10	473.42	13.52	277.14	196.28
	- Cl-D to Separator-02	9.37	23.84	0.74	26.20	270.74	12.38	127.93	142.81
2	**Steam (saturated)**								
	- Cl-C to interface point	7.90	4.11	1.05	40.00	141.28	30.60	108.08	33.20
	- Cl-D to interface point	8.29	4.30	0.74	40.00	74.61	25.62	47.79	26.82
3	**Brine**								
	- Cl-C to Cl-A	7.87	897.75	0.69	3.00	1017.91	1.52	516.42	501.49
	- Cl-D to Cl-F	8.29	895.51	0.39	3.00	316.50	1.90	200.56	115.95

Generally, Table 18 explains that the average fluid flow rate in the pipeline at the present conditions is only 60% of its maximum total capacity. Approximately 40% of the capacity in the pipeline can still be used for the future plans as described above. The schematic diagram in Figure 27 shows the possibility of a pipe tie-in from new makeup wells or an interconnection line from Unit-3 and Unit-4.

According to Figure 28, there are two possibilities of an interconnection line from Unit-3 and Unit-4 to Unit-1 and Unit-2. The first one is an interconnection of the two-phase line from Cluster-I to Cluster-B, as the pipes are close to each other, and each pipeline has a diameter of 36". Table 18 shows that the two-phase pipeline from Cluster-B can still accommodate 186.64 kg/s of two-phase fluid with a steam fraction of 19.41%. Similarly, through an interconnection line from Cluster-K to Cluster-D, it is still possible to accommodate 142.81 kg/s of two-phase fluid with a steam fraction of 19.75%. Line sizing

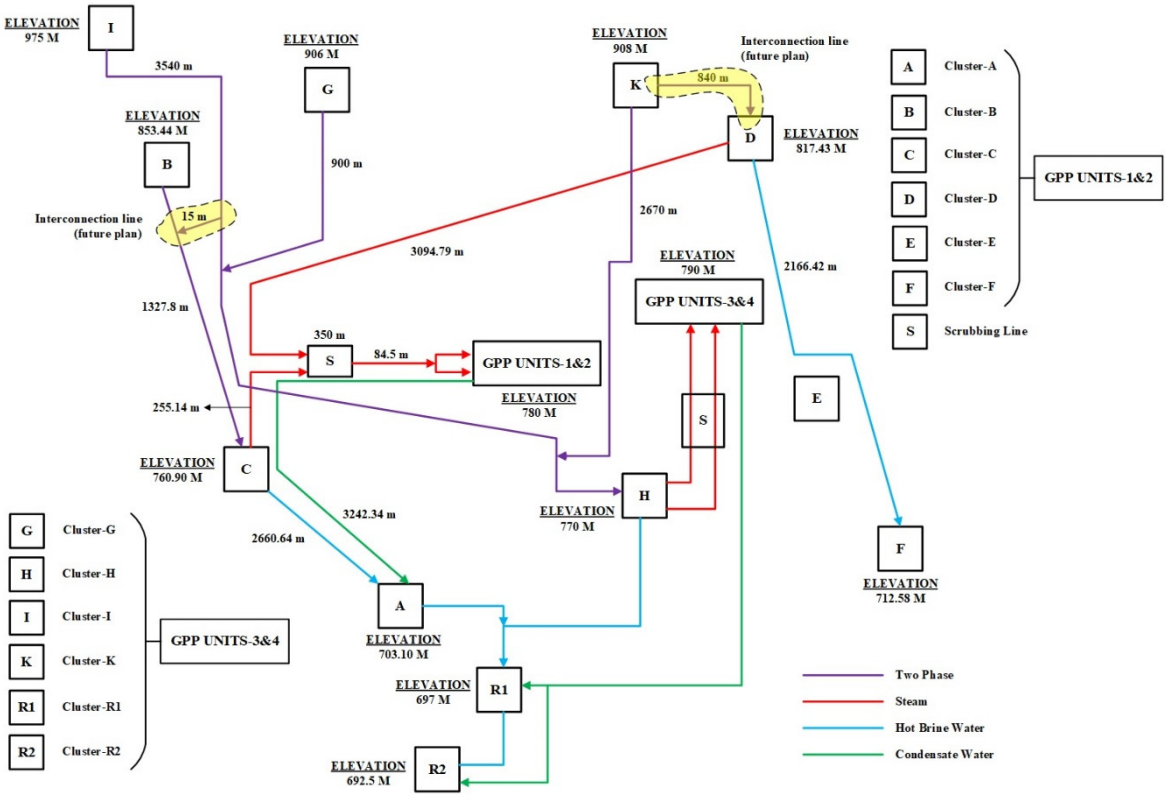

FIGURE 28: The schematic diagram of SAGS Unit-1 to Unit-4, Ulubelu, in correlation with future plans for a tie-in or an interconnection line from Units-3 and 4 to Units-1 and 2

related to the possibility of optimizing the flow in each pipeline depending on its services is displayed in Table 19.

TABLE 19: Sizing of pipelines in SAGS Unit-1 and Unit-2 for tie-in or interconnection between Units-3 and 4 and Units-1 and 2

No	Line service	Pressure (bar-a)	Density (kg/m^3)	Recommended maximum fluid velocity (m/s)	Possibility to optimize flow in the pipes (kg/s)	Line sizing		
						ID (m)	ID (“)	Selected DN (“)
1	**Two phase**							
	- Cl-B to Separator-01A	10.82	27.46	27.16	186.64	0.564	22.22	**24**
	- Cl-C to Separator-01B	8.88	32.67	23.10	196.28	0.576	22.66	**24**
	- Cl-D to Separator-02	9.37	23.84	26.20	142.81	0.540	21.24	**24**
2	**Steam (Saturated)**							
	- Cl-C to Interface Point	7.90	4.11	40.00	33.20	0.507	19.96	**20**
	- Cl-D to Interface Point	8.29	4.30	40.00	26.82	0.445	17.54	**18**
3	**Brine**							
	- Cl-C to Cl-A	7.87	897.75	3.00	501.49	0.487	19.17	**20**
	- Cl-D to Cl-F	8.29	895.51	3.00	115.95	0.234	9.23	**10**

4.7.4 Pressure profiling in the reinjection lines

Pressure profiling is done to determine the clogging of the reinjection lines due to silica scaling or other mineral deposition. Clogging of lines can be identified by comparing the theoretical pressure profile and the actual pressure profile of the system. Based on the calculation of pressure loss in the reinjection lines, which in this study are from the separators in Cluster-C and Cluster-D to the reinjection wells in Cluster-A and Cluster-F, we know the theoretical pressure profile along the pipelines. From the calculation of the SSI, it can be seen that there is potential of silica scaling in the reinjection line after Separator-02 in Cluster-D, so it is better to prioritize pressure profiling in this line. However, we don’t know the actual pressure profile since there are no pressure tapping points between the separator and the reinjection wells. Therefore, it is recommended to install some pressure tapping points between them. The selection of the location of the pressure tapping points should consider the pipeline configuration and elevation profile. Table 20 shows recommended sites for pressure tapping points on the reinjection line from Cluster-D to Cluster-F, while Figure 29 shows their location according to the elevation and length in a general pipe layout.

TABLE 20: Recommendation for the location of pressure tapping points in the reinjection line from Cluster-D to Cluster-F

No. of pressure tapping points	Elevation (m)	Length (m)	Remarks
1	815	40	The lowest point in Cluster-D after separator outlet of brine line
2	807	112	After downhill from Cluster-D
3	802	233	Before 1st expansion loop
4	782	447	Before 2nd expansion loop
5	764	630	Before 3rd expansion loop
6	747	859	After 4th expansion loop
7	737	1091	After 5th expansion loop and after elbow 45°
8	726	1209	After 6th expansion loop
9	723	1363	After 7th expansion loop
10	724	1409	After elbow 120°
11	723	1487	After 8th expansion loop
12	713	1773	After 9th expansion loop
13	713	1873	Before 10th expansion loop
14	714	1990	At box culvert
15	714	2082	After elbow 90° (near to Cluster-F)
16	713	2123	After elbow 90° (in Cluster-F)

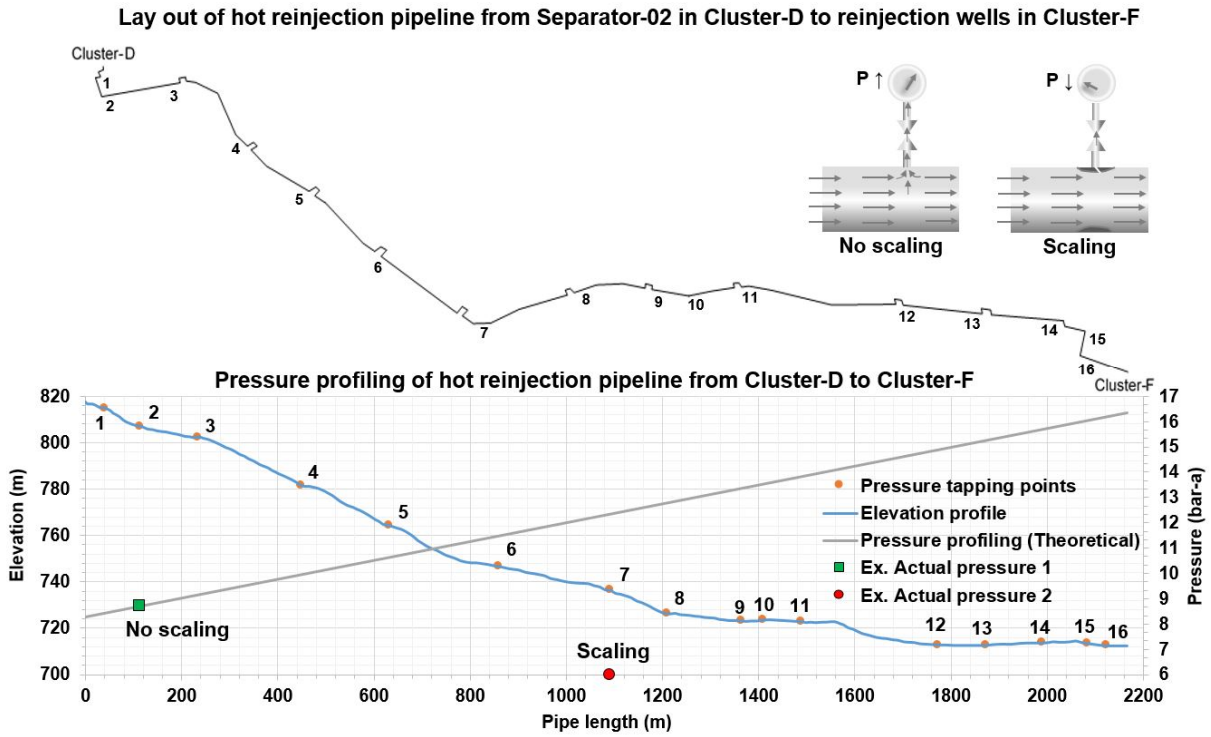

FIGURE 29: The location of pressure tapping points according to its elevation and length in general pipe lay out

It is recommended to use 1" diameter pipe nipples as tapping points. Since it is impossible to shut down the hot reinjection line, then hot tapping is worth considering for installation.

After the monitoring period of the pressure profiling on the reinjection line, the actual data must be plotted on a graph as shown in Figure 29, and compared to the theoretical pressure profiling. If significant differences are found between them, then it will be a special concern. Usually, an indication of clogging is characterized by a much smaller pressure for actual conditions than the theoretical pressure. This is because the nozzle of the pressure tapping is covered by silica scaling or mineral deposition in the pipe.

5. CONCLUSIONS

The assessment results in this study explain that the decline of operating parameters greatly affects the performance of the SAGS of Ulubelu Unit-1 and Unit-2. The total flow and pressure of the production wells is a very dominant parameter in influencing this, because it is an upstream input parameter of the SAGS that will determine the final condition in the downstream part. Due to the decrease of the total flow and pressure of the production wells, the pressure and total flow entering the separator has also decreased due to a pressure drop along the two-phase pipeline. The performance of the separators has also decreased as the input parameters decrease; this is indicated by the decrease of efficiency and steam quality at the outlet at the present conditions compared to the design conditions. In addition, there is an increase in the value of the silica saturation index in the brine line due to a decrease in the separator temperature. Also, in Separator-02 it is possible that silica scaling may have occurred at the current pressure and temperature conditions. In the steam line, the pressure at the interface point at present condition is already below the requirement agreed upon in the PJBU between PGE and PLN with the result that the power plant is operating at off-design conditions.

The pipes and separators of the SAGS have a decreased operating life after five years of operation. To analyse this, routine wall thickness measurements can be used as evaluation data. The results of the assessment show that there are several measurement points that have priority levels 1 and 2, meaning that the wall thickness may already be below allowable conditions. Consequently, it needs serious attention and action immediately.

In this study, several optimization scenarios are recommended to improve the performance of the SAGS in Ulubelu Unit-1 and Unit-2. A variation of separator pressure is worth consideration to increase the steam flow rate to the power plant. To increase the steam quality at the outlet, the steam velocity at separator inlet could be raised through a modification of the inlet pipe of the separator. Mapping of the pipeline capacity is also important for future strategies if new makeup wells are drilled, or interconnection lines between units in Ulubelu for the operational flexibility of the SAGS. Finally, pressure profiling in the reinjection line may determine location of silica scaling or other mineral depositions in the pipeline through monitoring at proposed pressure tapping points.

Finally it should be emphasized, that the calculations and analyses performed in this study are based on limited data and references. In addition, several assumptions are used to get these results. Therefore, before applying some of the above scenarios it is necessary to evaluate larger amount of data and a detailed and comprehensive analysis considering all aspects, including economic analysis and HSSE (health, safety, security and environment) aspects.

ACKNOWLEDGEMENTS

I would like to express my gratitude to Mr. Lúdvík S. Georgsson as Director of UNU-GTP Iceland and the management of PT Pertamina Geothermal Energy Indonesia, for giving me the opportunity to become one of the UNU-GTP fellows in 2017. Many thanks also to all staff of UNU GTP, Mr. Ingimar G. Haraldsson, Ms. Málfrídur Ómarsdóttir, Ms. Thórhildur Ísberg, and Mr. Markús A.G. Wilde for their care, advice and generous help.

I am also sincerely grateful to my supervisors, Dr. Páll Valdimarsson, Mr. Thorleikur Jóhannesson and Mr. Vigfús Arnar Jósefsson, for their guidance, advice, assistance and sharing of knowledge during the project.

Last but not least, big thanks to my family, especially to my parents, my dear wife and my children (including a new baby born last August) for their prayers, full support and patience during my six months in Iceland.

REFERENCES

API RP 14E, 1991: *Recommended practice for design and installation of offshore production platform piping system.* The American Petroleum Institute, Washington, DC, USA, 61 pp.

AS/NZS, 2006: *AS/NZS 3788-2006. Pressure equipment - in service inspection*. Australian Standard / New Zealand Standard, Sydney - Wellington, 205 pp.

ASME, 1995: *ASME 31.1-1995. Power piping*. The American Society of Mechanical Engineers, NY, USA, 366 pp.

Baker, O., 1954: Design of pipelines for simultaneous flow of oil and gas. *Oil and Gas J.*, *53*, 185-195.

Bangma, P., 1961: The development and performance of a steam-water separator for use on geothermal bores. *Proceedings of the UN Conference on New Sources of Energy, Vol. 2, Geothermal Energy Agenda, item II.A.2,* 60–77.

Bergthórsson, E.S., 2006: *Two-phase flow regimes and pressure drop in geothermal transmission pipes*. University of Iceland, Reykjavík, MSc thesis, 94 pp.

Chisholm, D., 1983: *Two-phase flow in pipelines and heat exchangers*. The Institution of Chemical Engineers, NY, 154-166.

Cooke, D.H., 1983: Modeling of off-design multistage turbine pressures by Stodola's ellipse. *Energy Inc. Pepse User's Group Meeting. 191-3*, 205-234.

Cruz, D.H., 2014: *SAGS assessment and evaluation*. PT Pertamina Geothermal Energy, Indonesia, unpublished lecture notes.

F-Chart Software, 2017: *EES, Engineering equation solver*. F-Chart Software internet website, *www.fchart.com/ees/.*

Fournier, R.O., and Rowe, J.J., 1977: The solubility of amorphous silica in water at high temperatures and high pressures. *Am. Min., 62,* 1052-1056.

Grant, M.A., Donaldson, I.G., and Bixley, P.F., 1982: *Geothermal reservoir engineering*. Academic Press, New York, 369 pp.

Hamrouni, B., and Dhahbi, M., 2001: Analytical aspects of silica in saline waters – application to desalination of brackish waters. *Desalination, 136*, 225-232.

Hoogendorn, C.J., 1959: Gas-liquid flow in horizontal pipes. *Chem. Engineering Science, 9-4*, 205-217.

IPS, 1996: *Engineering standard for process design of piping system*. Iranian Ministry of Petroleum, Tehran, Iran, 46 pp.

Lazalde-Crabtree, H., 1984: Design approach of steam-water separators and steam dryers for geothermal applications. *Geothermal Resource Council, Bulletin, September 1984*, 11–20.

Lawrence, E.A., 1952: Pressure loss in centrifugal entrainment separators under vacuum. *Chem. Eng. Prog., 48-5*, 241-246.

Leith, D., and Licht, W., 1972: The collection efficiency of cyclone type particle collectors: a new theoretical approach. *AICHE Symp. Ser., 68 (126)*, 196–206.

Ludwing, E.E., 1977: *Applied process design for chemical and petrochemical plants*. Gulf Publishing Co., Houston, TX, 646 pp.

Mandhane, J.M., Gregory, G.A., and Aziz, K., 1974: A flow pattern map for gas-liquid flow in horizontal pipes. *International J. Multiphase Flow, 1,* 537-553.

Mubarok, M.H. and Zarrouk, S.J., 2017: Discharge stimulation of geothermal wells: Overview and analysis. *Geothermics, 70*, 17-37.

Nukiyama, S. and Tanasawa, Y., 1938: Experiment on atomization of liquid by means of air stream, *Society of Mechanical Engineers, Trans., 4*, 86-93.

PGE, 2006: *Engineering, Procurement, Construction and Commissioning (EPCC) document of Steam above Ground System (SAGS) of Unit-2 and Unit-3 Lahendong geothermal field*. PT Pertamina Geothermal Energy Lahendong, Indonesia, unpublished report.

PGE, 2011: *Discharge test report of production wells in Ulubelu geothermal field*. PT Pertamina Geothermal Energy, Indonesia, unpublished report.

PGE, 2012: *Engineering, procurement, construction and commissioning (EPCC) document of steam above ground system (SAGS) of Unit-1 and Unit-2 Ulubelu geothermal field*. PT Pertamina Geothermal Energy Ulubelu, Indonesia, unpublished report.

PGE, 2017a: *Overview of Ulubelu geothermal field*. PT Pertamina Geothermal Energy Ulubelu, Indonesia, unpublished report.

PGE, 2017b: *Annual resource meeting*. PT Pertamina Geothermal Energy Ulubelu, Indonesia, unpublished report.

PGE, 2017c: *Geochemist laboratory analysis of Ulubelu geothermal field*. PT Pertamina Geothermal Energy Ulubelu, Indonesia, unpublished report.

Purwono, A.N., 2010: Comparison and selection of a steam gathering system in Ulubelu geothermal project, Sumatera, Indonesia. Report 26 in: *Geothermal training in Iceland 2010*. UNU-GTP, Iceland, 525-562.

Shepperd, C.B., and Lapple, C.E., 1939: Flow pattern and pressure drop in cyclone collectors. *Ind. Eng. Chem., 31*, 972-984.

Spedding, P.L., Cooper, R.K., and McBride, W.J., 2003: A universal flow regime map for horizontal two-phase flow in pipes. *Dev. Chem. Eng. Mineral Process, 11*, 95-106.

Spedding, P.L., and Spence, D.R., 1993: Flow regime in two-phase gas-liquid flow. *International J. Multiphase Flow, 19-2*, 245-280.

Spedding, P., and Watterson, J., 1998: Two-phase co-current flow in inclined pipe. *International J. of Heat and Mass Transfer, 41*, 4205-4228.

Whalley, P.B., 1987: *Boiling, condensation, and gas-liquid flow*. Clarendon Press, Oxford University Press, NY, 291 pp.

Wikipedia, 2017: *Ellipse law*. Wikipedia, website: *en.wikipedia.org/wiki/Ellipse_Law.*

Zhao, H.D., Lee, K.C., and Freeston, D.H. 2000: Geothermal two-phase flow in horizontal pipes. *Proceedings of the World Geothermal Congress 2000, Kyushu-Tohoku, Japan*, 3349-3352.

NOMENCLATURE

Alphabetic parameters

A = Total area (m^2);
A_e = Inlet width (m);
A_g = Area of steam (m^2);
A_{mc} = Thickness variation because of milling and corrosion (m);
A_o = Inlet area at cyclone wall (m^2);
AC = Acceleration correction;
B_e = Inlet height (m);
B_x, B_y = Baker's parameter at x-axis/y-axis, dimensionless;
C = Parameter defined by Equation 33**,** dimensionless;
D = Diameter of cyclone (m);
D_b = Water outlet pipe diameter (m);
D_e = Steam outlet pipe diameter (m);
D_o = Outer diameter of pipe (m);
D_S = Parameters that vary only with temperature and salt type;
D_T = Inlet pipe diameter (m);
d_w = Drop diameter (m);
E = Weld joint efficiency factor: 1, dimensionless;
f = Friction factor;
G = Mass fluxes of the gas phase;

H_f = Friction head (m of fluid);
h = Enthalpy (kJ/kg);
h_b = Equivalent length of bends, 20;
h_r = Equivalent length of reducer or other expansion units, 20;
h_v = Equivalent length of valves, 13;
h_M = Mixture enthalpy (kJ/kg);
h_{LS} = Water enthalpy (kJ/kg);
h_{VS} = Steam enthalpy (kJ/kg);
ID_{pipe} = Pipe inner diameter (m);
j = Parameter defined by Equation 48, dimensionless;
K_{BLO} = 1.6 *f h;*
K_C = Parameter defined by Equation 36, dimensionless;
L_P = Pipe length (m);
L = Mass fluxes of the liquid phase;
L_e = Length equivalent (m);
$\dot{m}$ = Total mass flow rate (kg/s);
$\dot{m}_g$ = Mass flow rate of steam (kg/s);
$\dot{m}_{01}$ = Off-design steam flow at inlet (kg/s);
n = Free vortex law coefficient, dimensionless;
n_1 = Parameter defined by Equation 30, dimensionless;
NH = Parameter defined by Equations 53 and 54, dimensionless;
OD_{pipe} = Pipe outer diameter (m);
P = Pressure (bar);
P_d = Design pressure (bar);
p_{01} = Pressure at inlet (bar);
p_{21} = Outlet pressure (bar);
Q_L = Volumetric water flow (m^3/s);
Q_{VS} = Volumetric steam flow (m^3/s);
r = Bend radius (m);
Re = Reynolds number, dimensionless;
S_h = Allowable stress of material at design temperature/hot stress (Pa);
s_o = Equilibrium solubility of silica in pure water;
s_{sat} = Corrected theoretical solubility of amorphous silica in water;
T = Temperature (°C);
T_{01} = Temperature inlet (°C);
t_{ma} = Maximum additional time of steam in cyclone (s);
t_{mi} = Average minimum residence time of steam in cyclone (s);
t_m = Requisite pipe thickness (m);
t_n = Nominal pipe thickness, commercial pipe thickness available (m);
t_{pipe} = Pipe thickness (m);
t_r = Residence time (s);
u = Inlet tangential velocity of drop at cyclone wall (m/s);
v = Velocity of fluid (m/s);
$\overline{V}_f$ = Average liquid phase velocity (m/s);
v_{AN} = Upward annular steam velocity (m/s);
V_L = Specific volume of water (m3/kg);
V_G = Specific volume of steam (m3/kg);
vo_H = Volume defined by Equation 41 (m);
vo_S = Volume defined by Equation 39 (m);
vo_1 = Volume defined by Equation 42 (m^3);
vo_2 = Volume defined by Equation 43 (m^3);
vo_3 = Volume defined by Equation 44 (m^3);
W_A = Mass flux of entrainment (kg/s);
W_L = Mass flux of water (kg/s);

W_M = Mass flux of inlet mixture (kg/s);
W_V = Mass flux of steam (kg/s);
x = Steam quality;
x_i = Inlet mixture quality, dimensionless
x_o = Outlet steam quality, dimensionless
y = Temperature dependent coefficient;
= 0.4 for steel with T < 482°C (Table 104.1.2(A) ASME B31.1);
z = Elevation (m);
1.1(1-*x*) = Correction factor mainly for the entrainment

Greek parameters
α = Void fraction;
ΔP = Pressure drop (bar);
ΔP_t = Total pressure drop (bar);
ΔP_f = Pressure drop due to friction (bar);
ΔP_{fi} = Pressure drop for installation (bar);
ΔP_L = Pressure drop due to length (bar);
ε = Absolute roughness of pipe (m);
ϵ_0 = Pressure ratios for design, dimensionless;
ϵ_{01} = Pressure ratios for off-design condition, dimensionless;
λ = Parameter, defined by Equation 13;
η_A = Entrainment efficiency, dimensionless
η_{ef} = Efficiency of separation, dimensionless
η_M = Centrifugal efficiency, dimensionless
μ = Dynamic viscosity of fluid (kg/ms);
μ_L = Water viscosity (kg/ms);
μ_V or μ_G = Steam viscosity (kg/ms);
Ψ = Centrifugal Inertial impaction parameter, defined by Equations 12 and 31, dimensionless;
ρ = Density of fluid (kg/m^3);
ρ_m = Density of mixture of water and steam (kg/m^3);
ρ_f or ρ_L = Density of water (kg/m^3);
ρ_V or ρ_G = Steam density (kg/m^3);
$\varphi^2_{BLO,b}$ = Two-phase multiplier for bends;
$\varphi^2_{BLO,r}$ = Two-phase multiplier for reducer or other expansions units;
$\varphi^2_{BLO,v}$ = Two-phase multiplier for valves.
σ_L = Surface tension of the liquid;

Abreviations
PJBL = Perjanjian Jual Beli Listrik or electricity sales contract;
PJBU = Perjanjian Jual Beli Uap or steam sales contract;
SAGS = Steam above ground system;
SSI = Silica saturation index;

APPENDIX I: The calculation flowchart of pressure drop in a two-phase line

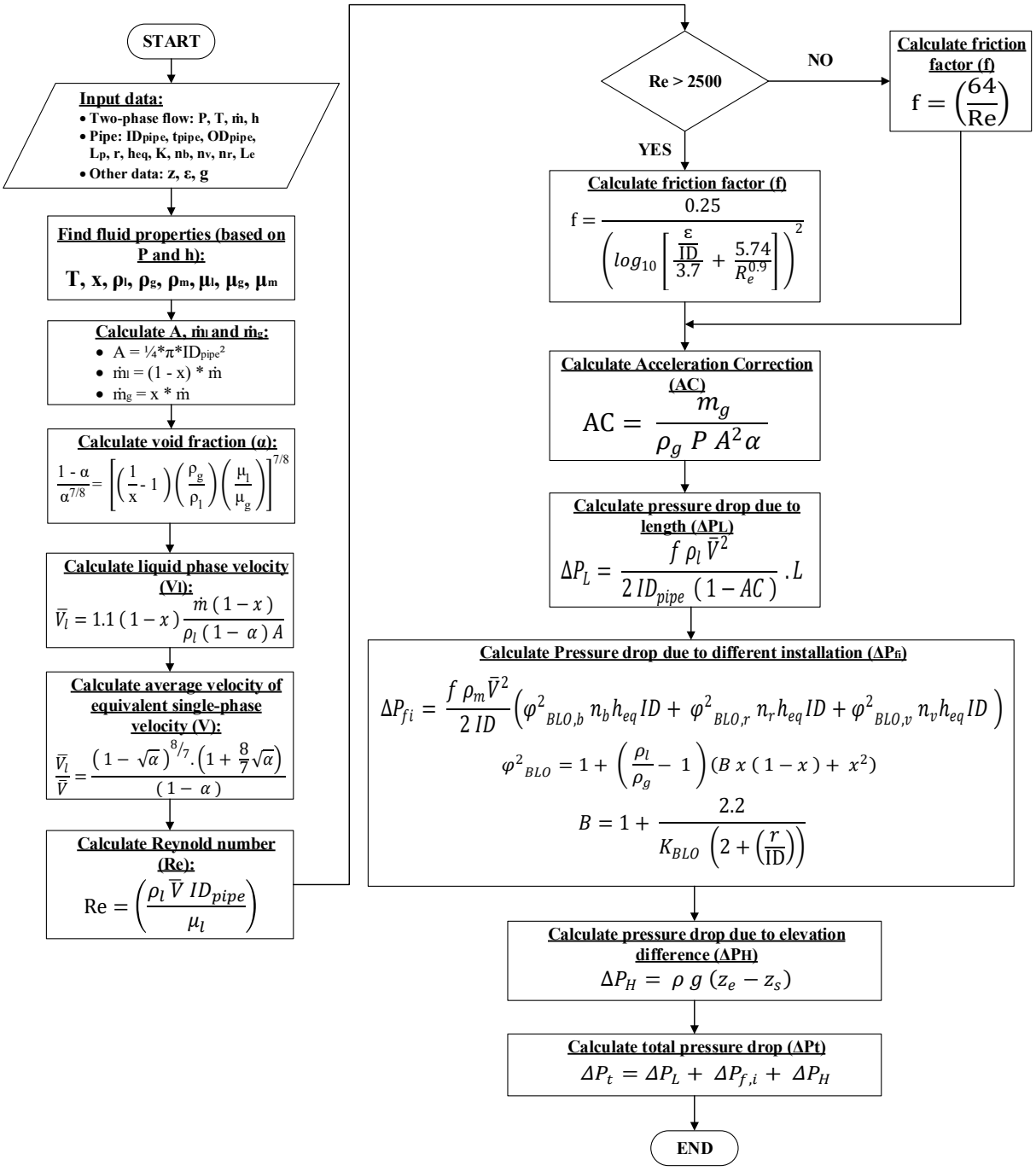

APPENDIX II: The example of two-phase flow pattern calculations in Cluster-B using EES

```
{!Input section}
{!++++++++++++++++++++++++++++++++++++++++++++++++++++++++++++++++++++++++++++++++++++++++++++++++++++++++++++++++}

"Baker and Mandhane et.al. two-phase flow patterns"

"Operation data"
"Cluster-B"
P_UBL_02 = 11.11                                    "Pressure after wellhead (Bara)"
m_dot_UBL_02 = 75.8                                 "Two phase flow from well (kg/s)"
h_UBL_02 = 1128.37                                  "Two phase enthalpy from well (kJ/kg)"

P_UBL_03 = 11.50                                    "Pressure after wellhead (Bara)"
m_dot_UBL_03 = 82.8                                 "Two phase flow from well (kg/s)"
h_UBL_03 = 1283.9                                   "Two phase enthalpy from well (kJ/kg)"

P_UBL_15 = 13.91                                    "Pressure after wellhead (Bara)"
m_dot_UBL_15 = 152.9                                "Two phase flow from well (kg/s)"
h_UBL_15 = 1201.74                                  "Two phase enthalpy from well (kJ/kg)"

P_UBL_16 = 18.92                                    "Pressure after wellhead (Bara)"
m_dot_UBL_16 = 14.3                                 "Two phase flow from well (kg/s)"
h_UBL_16 = 1361.19                                  "Two phase enthalpy from well (kJ/kg)"

"Two-phase pipeline data"
OD_pipe = 0.32385                                   "Outer dia. of 2-phase pipe from well to header, DN = 12in (m)"
t_pipe = 0.01748                                    "Pipe thickness SCH-80 (m)"
ID_pipe = OD_pipe-2*t_pipe                          "Inner dia. of 2-phase pipe from well to header, DN = 12in (m)"

{!Two-phase flow pattern calculation}
{!++++++++++++++++++++++++++++++++++++++++++++++++++++++++++++++++++++++++++++++++++++++++++++++++++++++++++++++++}
"Cluster-B"
P[1] = P_UBL_02
m_dot[1] = m_dot_UBL_02
h[1] = h_UBL_02

P[2] = P_UBL_03
m_dot[2] = m_dot_UBL_03
h[2] = h_UBL_03

P[3] = P_UBL_15
m_dot[3] = m_dot_UBL_15
h[3] = h_UBL_15

P[4] = P_UBL_16
m_dot[4] = m_dot_UBL_16
h[4] = h_UBL_16

Duplicate i=1,4
    T[i] = temperature(Water, P = P[i], x = 0)
    rho_v[i] = density(Water, P = P[i], x = 1)
    rho_l[i] = density(Water, P = P[i], x = 0)
    V_v[i] = 1/rho_v[i]
    V_l[i] = 1/rho_l[i]
    mu_v[i] = viscosity(Water, T = T[i], x = 1)
    mu_l[i] = viscosity(Water, T = T[i], x = 0)
    sigma_l[i] = surfacetension(Water, T = T[i])
    x[i] = quality(Water, P = P[i], h = h[i])
    Q[i] = m_dot[i]*3600

    Q_VS[i] = (Q[i]*x[i]*V_v[i])/3600
    Q_L[i] = (Q[i]*(1-x[i])*V_l[i])/3600


    "Baker Parameter (Bx and By)"
    Bx[i] = 4.499*((1-x[i])/x[i])*(rho_v[i]^0.5/rho_l[i]^0.167)*(mu_l[i]^0.333/sigma_l[i])
    By[i] = 7.086*(Q[i]*x[i])/((pi/4)*ID_pipe^2*(rho_l[i]*rho_v[i])^0.5)
```

```
"Modified Baker by Whalley (1987)"
psi[i] = (0.0724/sigma_l[i])*((mu_l[i]/0.0009)*(1000/rho_l[i])^2)^0.333333
lambda[i] = ((rho_v[i]/1.2)*(rho_l[i]/1000))^0.5
Bx_1[i] = (1-x[i])*(Q[i]/3600)*psi[i]
By_1[i] = x[i]*(Q[i]/3600)/lambda[i]

"Mandhane et.al. (1974) --> Superficial fluid velocity (ft/s)"
V_sl[i] = 3.28084*(4*Q_L[i])/(pi*ID_pipe^2)
V_sv[i] = 3.28084*(4*Q_VS[i])/(pi*ID_pipe^2)
End
```

Arrays Table: Main

	P_i	T_i	h_i	$\dot{m}_i$	x_i	$\rho_{l,i}$	$\rho_{v,i}$	$\mu_{l,i}$	$\mu_{v,i}$	Bx_i
1	11.11	184.5	1128	75.8	0.1727	882.2	5.689	0.0001463	0.00001518	21.26
2	11.5	186.1	1284	82.8	0.2478	880.5	5.88	0.000145	0.00001523	13.78
3	13.91	194.8	1202	152.9	0.1902	870.8	7.059	0.0001382	0.00001553	21.93
4	18.92	209.6	1361	14.3	0.2447	853.3	9.511	0.0001279	0.00001605	19.78

Arrays Table: Main

	By_i	$\sigma_{l,i}$	Q_i	$Q_{L,i}$	$Q_{VS,i}$	$V_{l,i}$	$V_{sl,i}$	$V_{sv,i}$	$V_{v,i}$
1	71901	0.04117	272880	0.07109	2.301	0.001134	3.558	115.2	0.1758
2	110966	0.04082	298080	0.07074	3.489	0.001136	3.541	174.6	0.1701
3	144346	0.03886	550440	0.1422	4.119	0.001148	7.117	206.2	0.1417
4	15114	0.03546	51480	0.01266	0.3678	0.001172	0.6336	18.41	0.1051

Arrays Table: Main

	λ_i	ψ_i	$Bx_{1,i}$	$By_{1,i}$
1	2.045	1.043	65.43	6.4
2	2.077	1.05	65.43	9.877
3	2.263	1.094	135.5	12.85
4	2.601	1.184	12.79	1.345

APPENDIX III: The results of wall thickness measurements in SAGS of Unit-1 and Unit-2 classified in the level of priority and action plan

No	Point no.	Line	Location	Size (inch)	Design pressure (Barg)	Pipe class	Corr. allow. - CA (mm)	Design thick. excl. CA (mm)	Design thick. incl. CA (mm)	Min. req'd. design thick. (mm)	Actual thickness measurement (mm)							Erosion / Corrosion rate, mm/year	Est. time to reach min. thickness, years	Action priority	Remarks
											13.mai.13	18.nóv.13	15.sep.14	12.jan.16	6.apr.16	24.jan.16	5.sep.16	5.jan.17			
1	02	Two-phase	Cluster-B	12	60.0	T3	3	17.48	20.48	12.66	18.36	16.41	10.11	16.19	17.37	18.11	17.22	18.07	0.0794	68.15	5	No significant metal loss noted. Monitor as required
2	03	Two-phase		12	60.0	T3	3	17.48	20.48	12.66	18.48	16.32	13.84	11.18	17.62	11.93	18.28	18.40	0.0603	95.25	5	No significant metal loss noted. Monitor as required
3	15	Two-phase		12	60.0	T3	3	17.48	20.48	12.66	18.27	16.33	13.95	16.89	17.26	14.57	17.12	18.38	0.3466	16.51	5	No significant metal loss noted. Monitor as required
4	16	Two-phase		12	60.0	T3	3	17.48	20.48	12.66	18.63	16.46	13.92	11.68	17.31	12.82	18.23	18.19	0.1205	45.92	5	No significant metal loss noted. Monitor as required
5	08	Two-phase		12	60.0	T3	3	17.48	20.48	12.66	18.40	16.46	14.13	9.46	9.46	18.05	18.05	18.05	0.0958	56.26	5	No significant metal loss noted. Monitor as required
6	05	Two-phase	Cluster-C	12	60.0	T3	3	17.48	20.48	12.66	18.45	15.51	13.71	9.10	17.40	18.19	18.19	18.19	0.0712	77.70	5	No significant metal loss noted. Monitor as required
7	06	Two-phase		12	60.0	T3	3	17.48	20.48	12.66	18.00	18.00	18.00	10.65	17.39	16.24	17.91	17.91	0.5645	9.30	4	Require regular monitoring
8	07	Two-phase		12	60.0	T3	3	17.48	20.48	12.66	18.37	14.40	14.20	11.19	17.78	17.78	18.27	17.82	0.1506	34.28	5	No significant metal loss noted. Monitor as required
9	12	Two-phase		12	60.0	T3	3	17.48	20.48	12.66	18.28	16.18	13.47	16.64	16.86	17.82	17.56	17.45	0.2273	21.09	5	No significant metal loss noted. Monitor as required
10	11	Two-phase	Cluster-D	12	60.0	T3	3	17.48	20.48	12.66	19.77	17.15	12.47	19.01	18.30	12.63	18.20	17.62	0.5887	8.43	4	Require regular monitoring
11	14	Two-phase		12	60.0	T3	3	17.48	20.48	12.66	18.00	16.30	16.30	16.30	16.30	16.30	18.28	18.28	0.5453	10.31	5	No significant metal loss noted. Monitor as required
12	B-C 01	Two-phase		36	12.8	T1	3	10.31	13.31	9.70	13.03	11.96	10.50	10.74	10.82	10.36	10.88	10.78	0.6161	1.75	3	High corrosion rate. Require regular monitoring.
13	B-C 02	Two-phase		36	12.8	T1	3	10.31	13.31	9.70	13.16	12.18	10.55	11.49	10.67	10.68	12.25	10.55	0.7147	1.19	3	High corrosion rate. Require regular monitoring.
14	B-C 03	Two-phase		36	12.8	T1	3	10.31	13.31	9.70	13.19	11.50	10.40	11.10	10.88	11.51	10.90	10.49	0.7393	1.07	3	High corrosion rate. Require regular monitoring.
15	B-C 04	Two-phase		36	12.8	T1	3	10.31	13.31	9.70	13.06	11.90	10.22	11.06	10.85	12.40	10.46	10.82	0.6134	1.82	3	High corrosion rate. Require regular monitoring.
16	B-C 05	Two-phase	Cluster-B to Cluster-C	36	12.8	T1	3	10.31	13.31	9.70	11.23	11.30	10.62	11.31	10.77	11.03	11.21	10.80	0.1177	9.33	4	Require regular monitoring
17	B-C 06	Two-phase		36	12.8	T1	3	10.31	13.31	9.70	13.14	11.71	10.49	11.10	10.75	11.35	11.05	10.80	0.6407	1.72	3	High corrosion rate. Require regular monitoring.
18	B-C 07	Two-phase		36	12.8	T1	3	10.31	13.31	9.70	13.08	11.80	10.73	11.04	10.68	11.35	11.11	10.97	0.5778	2.20	3	High corrosion rate. Require regular monitoring.
19	B-C 08	Two-phase		36	12.8	T1	3	10.31	13.31	9.70	13.06	12.35	10.40	11.01	10.93	11.21	11.55	10.77	0.6270	1.70	3	High corrosion rate. Require regular monitoring.
20	B-C 09	Two-phase		36	12.8	T1	3	10.31	13.31	9.70	13.12	12.35	10.40	10.67	10.82	10.05	10.85	10.82	0.6298	1.78	3	High corrosion rate. Require regular monitoring.
21	01A-01	Separator	Cluster-C	103.28	13.8		3	18.00	21.00	15.90	19.74	No measurement data						18.64	0.3012	9.10	4	Require regular monitoring
22	01A-02	Separator		103.28	13.8		3	18.00	21.00	15.90	19.95							19.41	0.1479	23.74	5	No significant metal loss noted. Monitor as required
23	01B-01	Separator		103.28	13.8		3	18.00	21.00	15.90	19.85							18.40	0.3957	6.32	4	Require regular monitoring
24	01B-02	Separator		103.28	13.8		3	18.00	21.00	15.90	19.93							18.55	0.3776	7.02	4	Require regular monitoring
25	02-01	Separator	Cluster-D	103.28	17.6		3	20.00	23.00	19.50	21.62							20.24	0.3779	1.96	3	High corrosion rate. Require regular monitoring.
26	02-02	Separator		103.28	17.6		3	20.00	23.00	19.50	21.74							20.38	0.3710	2.37	3	High corrosion rate. Require regular monitoring.
27	C-PP 01	Steam	Cluster-C to Header in interface point area	42	10.8	S1	3	10.31	13.31	9.61	13.65	12.14	11.42	11.10	10.57	13.34	11.21	10.54	0.8516	1.09	3	High corrosion rate. Require regular monitoring.
28	C-PP 02	Steam		48	10.8	S1	3	11.13	14.13	10.49	13.14	12.02	12.02	10.12	11.45	10.98	10.44	11.47	0.4573	2.14	3	High corrosion rate. Require regular monitoring.
29	C-PP 03	Steam		28	10.8	S1	3	9.53	12.53	8.57	12.02	11.04	11.04	11.42	9.37	10.62	10.59	11.59	0.1177	25.62	5	No significant metal loss noted. Monitor as required
30	C-PP 04	Steam		48	10.8	S1	3	11.13	14.13	10.49	13.49	11.04	11.04	11.01	11.51	10.23	11.44	11.49	0.5476	1.82	3	High corrosion rate. Require regular monitoring.
31	C-PP 05	Steam		48	10.8	S1	3	11.13	14.13	10.49	13.16	11.25	11.25	10.20	11.48	10.67	11.37	9.12	1.1062	-1.24	1	Remaining pipe thickness less than design minimum requirement. Require immediate replacement or line to be derated
32	C-PP 06	Steam		52	10.8	S1	3	11.13	14.13	11.08	13.17	11.45	11.45	11.10	9.76	11.35	11.45	9.75	0.9365	-1.42	1	Remaining pipe thickness less than design minimum requirement. Require immediate replacement or line to be derated
33	C-PP 07	Steam		40	10.8	S1	3	9.53	12.53	9.31	12.15	11.30	11.30	11.12	9.78	11.30	11.53	10.81	0.3669	4.08	3	High corrosion rate. Require regular monitoring.
34	C-PP 08	Steam		40	10.8	S1	3	9.53	12.53	9.31	12.13	11.30	11.30	11.25	9.71	12.21	10.89	9.29	0.7776	-0.03	1	Remaining pipe thickness less than design minimum requirement. Require immediate replacement or line to be derated
35	D-PP 01	Steam		30	12.0	S1	3	9.53	12.53	8.94	12.24	10.90	12.17	10.99	9.73	10.11	11.14	9.14	0.8488	0.24	2	Corrosion rate too high. To be verified and closely monitored. Replacement to be done within one year or line derated to safe design condition if wall thickness falls below original design parameters.
36	D-PP 02	Steam		30	12.0	S1	3	9.53	12.53	8.94	18.23	15.10	12.19	16.63	17.41	16.32	11.53	17.43	0.2191	38.76	5	No significant metal loss noted. Monitor as required
37	D-PP 03	Steam		30	12.0	S1	3	9.53	12.53	8.94	12.26	11.15	8.75	10.37	9.15	10.18	10.47	9.75	0.6873	1.18	3	High corrosion rate. Require regular monitoring.

38	D-PP 04	Steam	Cluster-D to Header in interface point area	30	12.0	S1	3	9.53	12.53	8.94	12.00	11.34	8.63	10.44	9.21	10.65	17.22	9.11	0.7913	0.21	2	Corrosion rate too high. To be verified and closely monitored. Replacement to be done within one year or line derated to safe design condition if wall thickness falls below original design parameters.
39	D-PP 05	Steam		30	12.0	S1	3	9.53	12.53	8.94	12.35	11.18	9.04	10.72	9.85	10.46	10.40	9.70	0.7256	1.05	3	High corrosion rate. Require regular monitoring.
40	D-PP 06	Steam		30	12.0	S1	3	9.53	12.53	8.94	12.47	10.95	8.03	10.23	9.33	10.13	10.77	9.67	0.7667	0.95	2	Corrosion rate too high. To be verified and closely monitored. Replacement to be done within one year or line derated to safe design condition if wall thickness falls below original design parameters.
41	D-PP 07	Steam		30	12.0	S1	3	9.53	12.53	8.94	12.17	11.09	8.51	11.10	9.75	10.15	10.27	9.80	0.6489	1.33	3	High corrosion rate. Require regular monitoring.
42	D-PP 08	Steam		30	12.0	S1	3	9.53	12.53	8.94	12.27	11.10	8.42	10.92	9.69	10.09	10.86	9.22	0.8351	0.34	2	Corrosion rate too high. To be verified and closely monitored. Replacement to be done within one year or line derated to safe design condition if wall thickness falls below original design parameters.
43	D-PP 09	Steam		30	12.0	S1	3	9.53	12.53	8.94	12.29	11.00	8.50	10.88	9.77	10.23	10.40	9.70	0.7092	1.07	3	High corrosion rate. Require regular monitoring.
44	D-PP 10	Steam		30	12.0	S1	3	9.53	12.53	8.94	12.21	11.09	8.57	10.69	9.76	10.31	10.77	9.77	0.6681	1.24	3	High corrosion rate. Require regular monitoring.
45	D-PP 11	Steam		30	12.0	S1	3	9.53	12.53	8.94	12.20	10.90	8.35	11.10	9.71	10.88	10.61	9.62	0.7065	0.96	2	Corrosion rate too high. To be verified and closely monitored. Replacement to be done within one year or line derated to safe design condition if wall thickness falls below original design parameters.
46	D-PP 12	Steam		30	12.0	S1	3	9.53	12.53	8.94	12.04	11.00	8.32	10.43	9.75	11.32	10.77	9.28	0.7557	0.45	2	Corrosion rate too high. To be verified and closely monitored. Replacement to be done within one year or line derated to safe design condition if wall thickness falls below original design parameters.
47	D-PP 13	Steam		30	12.0	S1	3	9.53	12.53	8.94	12.24	10.80	9.81	10.29	10.10	10.06	10.90	9.69	0.6982	1.07	3	High corrosion rate. Require regular monitoring.
48	D-PP 14	Steam		30	12.0	S1	3	9.53	12.53	8.94	12.33	11.12	10.31	10.89	10.04	10.64	10.90	9.71	0.7174	1.07	3	High corrosion rate. Require regular monitoring.
49	D-PP 15	Steam		30	12.0	S1	3	9.53	12.53	8.94	12.12	10.95	9.91	10.99	10.04	11.27	10.85	9.78	0.6407	1.31	3	High corrosion rate. Require regular monitoring.
50	D-PP 16	Steam		30	12.0	S1	3	9.53	12.53	8.94	12.12	11.04	10.03	9.65	9.23	10.36	11.10	9.77	0.6435	1.29	3	High corrosion rate. Require regular monitoring.
51	D-PP 17	Steam		30	12.0	S1	3	9.53	12.53	8.94	12.52	11.03	10.33	10.02	9.72	10.17	10.10	9.65	0.7859	0.90	2	Corrosion rate too high. To be verified and closely monitored. Replacement to be done within one year or line derated to safe design condition if wall thickness falls below original design parameters.
52	D-PP 18	Steam		30	12.0	S1	3	9.53	12.53	8.94	12.23	10.85	10.35	9.12	11.29	10.44	10.74	9.73	0.6845	1.15	3	High corrosion rate. Require regular monitoring.
53	D-PP 19	Steam		30	12.0	S1	3	9.53	12.53	8.94	12.32	12.06	10.40	10.06	11.39	11.31	10.76	9.79	0.6928	1.23	3	High corrosion rate. Require regular monitoring.
54	D-PP 20	Steam		30	12.0	S1	3	9.53	12.53	8.94	12.25	11.98	10.69	10.82	11.26	12.06	12.06	11.10	0.3149	6.86	4	Require regular monitoring
55	C-A 01	Hot brine water	Cluster-C to Cluster-A	28	13.4	B2	3	8.74	11.74	8.54	11.68	11.01	10.07	9.44	9.10	9.71	9.19	8.21	0.9502	-0.34	1	Remaining pipe thickness less than design minimum requirement. Require immediate replacement or line to be derated
56	C-A 02	Hot brine water		28	13.4	B2	3	8.74	11.74	8.54	11.85	11.04	10.00	9.36	9.36	9.23	9.22	8.19	1.0022	-0.34	1	Remaining pipe thickness less than design minimum requirement. Require immediate replacement or line to be derated
57	C-A 03	Hot brine water		28	13.4	B2	3	8.74	11.74	8.54	11.99	10.96	9.90	9.08	9.15	10.02	10.04	9.23	0.7557	0.92	2	Corrosion rate too high. To be verified and closely monitored. Replacement to be done within one year or line derated to safe design condition if wall thickness falls below original design parameters.
58	C-A 04	Hot brine water		28	13.4	B2	3	8.74	11.74	8.54	11.97	10.89	9.86	9.10	9.21	10.09	9.25	9.31	0.7284	1.06	3	High corrosion rate. Require regular monitoring.
59	C-A 05	Hot brine water		28	13.4	B2	3	8.74	11.74	8.54	11.88	11.17	9.87	9.29	9.12	10.08	9.25	9.28	0.7119	1.05	3	High corrosion rate. Require regular monitoring.
60	C-A 06	Hot brine water		28	13.4	B2	3	8.74	11.74	8.54	12.00	11.15	9.80	9.31	10.36	9.87	9.46	9.15	0.7804	0.79	2	Corrosion rate too high. To be verified and closely monitored. Replacement to be done within one year or line derated to safe design condition if wall thickness falls below original design parameters.
61	C-A 07	Hot brine water		28	13.4	B2	3	8.74	11.74	8.54	11.84	11.05	9.70	9.44	9.30	10.05	9.37	9.16	0.7338	0.85	2	Corrosion rate too high. To be verified and closely monitored. Replacement to be done within one year or line derated to safe design condition if wall thickness falls below original design parameters.
62	C-A 08	Hot brine water		28	13.4	B2	3	8.74	11.74	8.54	11.96	11.15	9.85	9.21	10.14	10.31	9.04	9.27	0.7366	1.00	2	Corrosion rate too high. To be verified and closely monitored. Replacement to be done within one year or line derated to safe design condition if wall thickness falls below original design parameters.

63	C-A 09	Hot brine water		28	13.4	B2	3	8.74	11.74	8.54	12.02	11.13	10.01	9.21	9.31	10.11	10.11	9.19	0.7749	0.85	2	Corrosion rate too high. To be verified and closely monitored. Replacement to be done within one year or line derated to safe design condition if wall thickness falls below original design parameters.
64	C-A 10	Hot brine water		28	13.4	B2	3	8.74	11.74	8.54	11.85	10.74	9.70	9.90	9.22	10.12	9.18	9.24	0.7147	0.99	2	Corrosion rate too high. To be verified and closely monitored. Replacement to be done within one year or line derated to safe design condition if wall thickness falls below original design parameters.
65	C-A 11	Hot brine water		28	13.4	B2	3	8.74	11.74	8.54	11.95	11.00	9.65	9.27	9.24	10.24	9.56	9.26	0.7366	0.98	2	Corrosion rate too high. To be verified and closely monitored. Replacement to be done within one year or line derated to safe design condition if wall thickness falls below original design parameters.
66	D-F 01	Hot brine water		20	20.4	B2	3	9.53	12.53	8.97	12.33	11.13	8.63	10.26	10.01	10.27	10.12	9.24	0.8461	0.32	2	Corrosion rate too high. To be verified and closely monitored. Replacement to be done within one year or line derated to safe design condition if wall thickness falls below original design parameters.
67	D-F 02	Hot brine water		20	20.4	B2	3	9.53	12.53	8.97	12.26	10.96	8.47	10.01	9.70	10.32	10.25	9.80	0.6736	1.24	3	High corrosion rate. Require regular monitoring.
68	D-F 03	Hot brine water		20	20.4	B2	3	9.53	12.53	8.97	12.32	10.93	8.44	10.42	9.73	10.04	9.90	9.65	0.7311	0.93	2	Corrosion rate too high. To be verified and closely monitored. Replacement to be done within one year or line derated to safe design condition if wall thickness falls below original design parameters.
69	D-F 04	Hot brine water		20	20.4	B2	3	9.53	12.53	8.97	12.48	11.31	8.47	9.68	9.78	9.98	9.50	9.79	0.7366	1.12	3	High corrosion rate. Require regular monitoring.
70	D-F 05	Hot brine water		20	20.4	B2	3	9.53	12.53	8.97	12.32	11.00	8.35	10.25	10.15	10.13	9.55	9.83	0.6818	1.27	3	High corrosion rate. Require regular monitoring.
71	D-F 06	Hot brine water		20	20.4	B2	3	9.53	12.53	8.97	12.33	10.97	8.46	10.37	9.83	9.09	9.36	9.35	0.8160	0.47	2	Corrosion rate too high. To be verified and closely monitored. Replacement to be done within one year or line derated to safe design condition if wall thickness falls below original design parameters.
72	D-F 07	Hot brine water	Cluster-D to Cluster-F	20	20.4	B2	3	9.53	12.53	8.97	12.74	11.54	8.79	9.57	9.81	10.24	9.81	10.25	0.6818	1.88	3	High corrosion rate. Require regular monitoring.
73	D-F 08	Hot brine water		20	20.4	B2	3	9.53	12.53	8.97	12.26	11.08	8.55	10.47	9.81	10.06	9.54	9.28	0.8160	0.38	2	Corrosion rate too high. To be verified and closely monitored. Replacement to be done within one year or line derated to safe design condition if wall thickness falls below original design parameters.
74	D-F 09	Hot brine water		20	20.4	B2	3	9.53	12.53	8.97	12.28	11.02	8.60	10.64	9.79	10.00	10.01	9.22	0.8379	0.30	2	Corrosion rate too high. To be verified and closely monitored. Replacement to be done within one year or line derated to safe design condition if wall thickness falls below original design parameters.
75	D-F 10	Hot brine water		20	20.4	B2	3	9.53	12.53	8.97	12.30	11.09	8.74	10.82	9.83	10.24	9.48	9.77	0.6928	1.16	3	High corrosion rate. Require regular monitoring.
76	D-F 11	Hot brine water		20	20.4	B2	3	9.53	12.53	8.97	12.44	11.01	8.51	9.81	9.04	10.05	9.73	9.72	0.7448	1.01	3	High corrosion rate. Require regular monitoring.
77	D-F 12	Hot brine water		20	20.4	B2	3	9.53	12.53	8.97	12.36	10.98	8.62	10.22	9.80	10.18	9.41	9.81	0.6982	1.21	3	High corrosion rate. Require regular monitoring.
78	D-F 13	Hot brine water		20	20.4	B2	3	9.53	12.53	8.97	12.34	11.36	8.68	10.01	9.09	10.46	9.57	9.81	0.6928	1.22	3	High corrosion rate. Require regular monitoring.
79	D-F 14	Hot brine water		20	20.4	B2	3	9.53	12.53	8.97	12.21	10.32	8.79	10.51	9.10	10.23	9.01	9.75	0.6736	1.16	3	High corrosion rate. Require regular monitoring.
80	01	Hot brine water	Cluster-A	12	13.4	B2	3	9.53	12.53	6.96	12.37	11.13	9.70	10.14	9.80	11.58	10.22	10.42	0.5339	6.48	4	Require regular monitoring
81	18	Hot brine water		12	13.4	B2	3	9.53	12.53	6.96	12.26	11.10	10.01	8.79	9.78	12.52	10.32	10.32	0.5312	6.33	4	Require regular monitoring
82	21	Hot brine water		12	20.4	B2	3	9.53	12.53	6.96	12.36	11.09	8.37	8.37	10.58	10.93	9.70	9.82	0.6955	4.11	3	High corrosion rate. Require regular monitoring.
83	19	Hot brine water	Cluster-F	12	20.4	B2	3	9.53	12.53	6.96	12.56	11.18	8.80	8.80	10.43	10.23	9.80	9.80	0.7557	3.76	3	High corrosion rate. Require regular monitoring.
84	17	Hot brine water		12	20.4	B2	3	9.53	12.53	6.96	12.03	10.95	8.04	8.59	11.10	10.17	9.09	9.09	0.8050	2.65	3	High corrosion rate. Require regular monitoring.

Action Priority No.

1 Program replacement immediately or derate line to suit the max. expected current operating conditions.
2 Program replacement in less than a year and require close monitoring.
3 Program replacement in 1 to 5 years require regular monitoring.
4 Program replacement in 5 to 10 years
5 Expected life before failure is beyond 10 years